Supporting Information

Micro-Changes, Macro-Impact: Enhancing Hole Transfer by Tailoring Peripheral Substituents of Hole Transport Materials for Efficient Perovskite Solar Cells

Ziyang Xia,[a,b] Xuezhen Feng,[c] Cheng Chen,*[a] Bin Cai,[a] Linqin Wang,[d] Mengde Zhai,[a] Xue Lou,[e] Sang Il Seok,*[b] Ming Cheng*[a]

[a] Institute for Energy Research, Jiangsu University, Zhenjiang 212013, China.

[b] Department of Energy Engineering, School of Energy and Chemical Engineering, Ulsan National Institute of Science and Technology (UNIST), Ulsan, 44919 South Korea.

[c] Shenzhen Key Laboratory of Interfacial Science and Engineering of Materials (SKLISEM), School of Environmental Science and Engineering, Southern University of Science and Technology, Shenzhen 518055, China.

[d] Center of Artificial Photosynthesis for Solar Fuels, School of Science, Westlake University, Hangzhou 310024, China.

[e] Instrumentation and service center for molecular sciences, Westlake University, Hangzhou 310030, China.

Supporting Information

1. Synthesis of Hole Transport Materials.

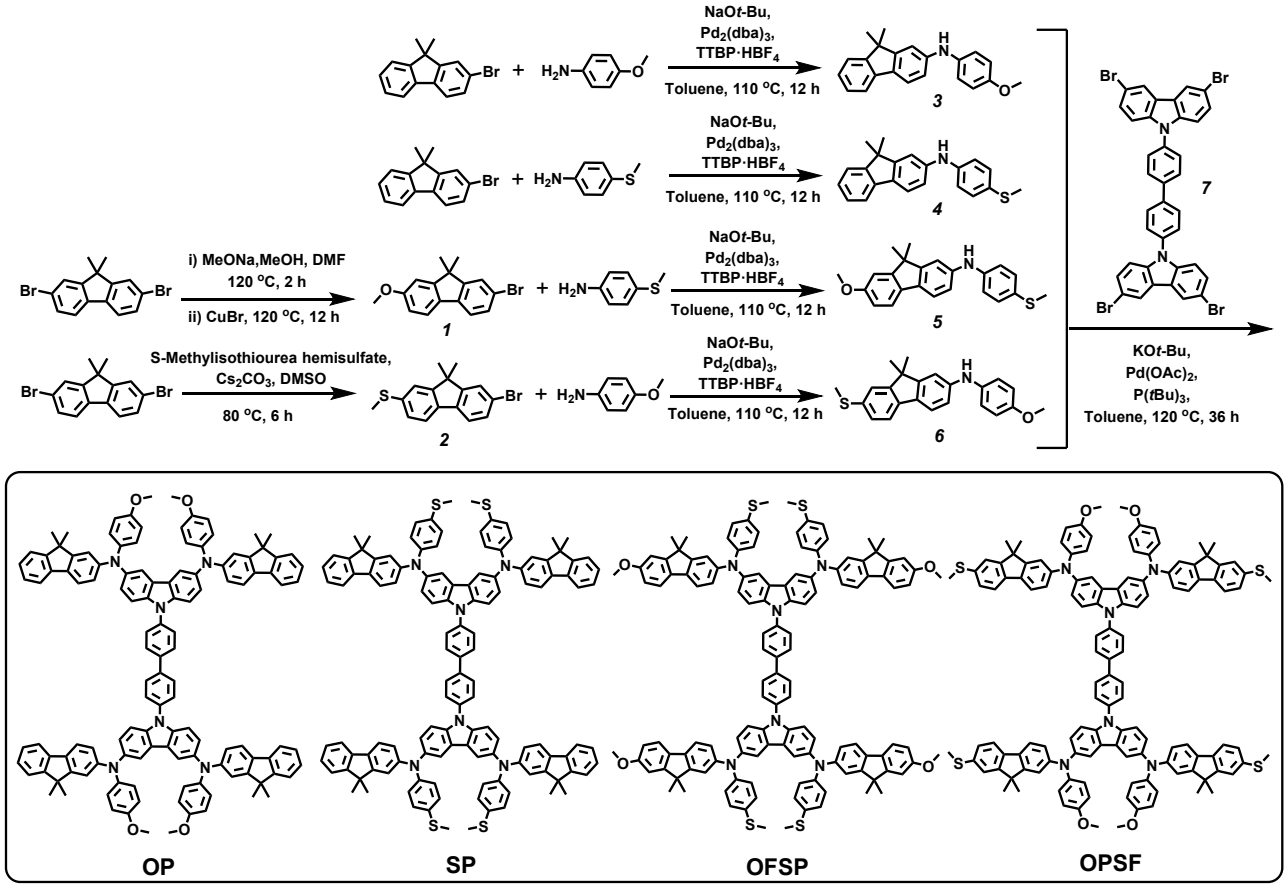

Scheme S1. The detailed synthetic route and chemical structure of **OP**, **SP**, **OFSP** and **OPSF**.

1.1 Reagents and Solvents.

All reagents and solvents were purchased from commercial sources without any further purification and dried according to standard procedures. 2-Bromo-9,9′-dimethylfluorene (98%, Energy Chemical), 2,7-Dibromo-9,9-dimethylfluorene (98%, Energy Chemical), 4-Methoxyaniline (99%, Energy Chemical), 4-(Methylthio)aniline (98%, Energy Chemical), Sodium tert-butoxide (NaO*t*-Bu, 98%, Energy Chemical), Carbazole (97%, Aladdin), 4,4′-Diiodo-1,1′-biphenyl (99%, Energy Chemical), Tris(dibenzylideneacetone)dipalladium ($Pd_2(dba)_3$, 99%, Aladdin), Palladium acetate ($Pd(OAc)_2$, 98%, Aladdin), Potassium tert-butoxide (KO*t*-Bu, 98%, Aladdin), *S*-Methylisothiourea hemisulfate (98%, Energy Chemical), Sodium methoxide (MeONa, 95%, Energy

Chemical), P(*t*Bu)$_3$ (10% in Toluene, Aladdin), Tri-tert-butylphosphonium (TTBP·HBF$_4$, 98%, Energy Chemical), Toluene (99.5%, Sinopharm Chemical), Dimethyl sulfoxide (DMSO, 99.8%, Energy Chemical).

1.2 Details.

The compound **3** and **7** were synthesized according to previously reported method.[1-2]

*2-bromo-7-methoxy-9,9-dimethyl-9H-fluorene (**1**)*: 2,7-Dibromo-9,9-dimethylfluorene (2.00 g, 5.68 mmol) was added into 10 mL dry DMF in 50 mL two-necked flask. The mixture was purged with nitrogen for 20 min, and the reaction was stirred at 120 ℃, and then the solution of MeONa (10 mL, 0.31 g/mL in MeOH, 57.39 mmol) was dropwised to the reaction system. Subsequently, the reaction was kept at the same temperature for 2 h, then CuBr (0.08 g, 0.57 mmol) was added to the reaction system and continued for 12 h. After reaction, cool the solution to room temperature, it was then extracted with ethyl acetate, the two phases were separated, and the water phase was extracted twice with ethyl acetate. The combined organic extracts were washed three times with water, dried over Na_2SO_4, evaporated, purified with column chromatography (eluting with petroleum ether / ethyl acetate, 15/1 v/v) and dried under vacuum to obtain the compound ***1*** as a white power (1.15 g, 3.82 mmol, 67.3% yield). ^{1}H NMR (400 MHz, $CDCl_3$-*d*) δ = 7.59 (d, *J*=8.3, 1H), 7.53 – 7.46 (m, 2H), 7.43 (dd, *J*=8.0, 1.8, 1H), 6.96 (d, *J*=2.4, 1H), 6.89 (dd, *J*=8.3, 2.4, 1H), 3.88 (s, 3H).

*(7-bromo-9,9-dimethyl-9H-fluoren-2-yl)(methyl)sulfane (**2**)*: A mixture of 2,7-Dibromo-9,9-dimethylfluorene (5.25 g, 15 mmol), *S*-Methylisothiourea hemisulfate (4.17 g, 30 mmol), cesium carbonate (19.55 g, 60 mmol) were added into 25 mL dry DMSO in 50 mL two-necked flask, and the reaction was stirred at 80 ℃ for 6 h. After completion of the reaction, the mixture was poured into water and extracted with ethyl acetate (3 × 15 mL). The combined organic layers were dried over

anhydrous Na_2SO_4 and filtered. After the removal of the solvent, the residue was directly used for purified by flash column chromatography on silica gel using petroleum ether / ethyl acetate (10/1 v/v) as the eluent to afford the compound ***2*** as white power (3.71 g, 11.66 mmol, 78.2% yield). ^{1}H NMR (400 MHz, $CDCl_3$-*d*) δ = 7.60 (d, *J*=8.0, 1H), 7.56 – 7.50 (m, 2H), 7.45 (dd, *J*=8.1, 1.8, 1H), 7.33 (d, *J*=1.8, 1H), 7.24 (dd, *J*=8.0, 1.8, 1H), 2.56 (s, 3H), 1.47 (s, 6H).

9,9-dimethyl-N-(4-(methylthio)phenyl)-9H-fluoren-2-amine ***(4)***: 2-Bromo-9,9′-dimethylfluorene (5.46 g, 20 mmol), 4-(Methylthio)aniline (4.18 g, 30 mmol), $Pd_2(dba)_3$ (0.92 g, 1 mmol), and NaO*t*-Bu (5.77 g, 60 mmol) were added into 80 mL dry toluene in 250 mL two-necked flask. The mixture was purged with nitrogen for 20 min, then TTBP·HBF_4 (0.58 g, 2 mmol) was further added into the mixture solution, and the reaction was stirred at 110 ℃ for 12 h. After reaction, cool the solution to room temperature, it was then extracted with dichloromethane, the two phases were separated, and the water phase was extracted twice with dichloromethane. The combined organic extracts were washed three times with water, dried over Na_2SO_4, evaporated, purified with column chromatography (eluting with petroleum ether / dichloromethane, 2/1 v/v) and dried under vacuum to obtain the compound ***4*** as a white power (5.51 g, 16.62 mmol, 83.1% yield). ^{1}H NMR (400 MHz, DMSO-d_6) δ = 8.33 (s, 1H), 7.64 (d, *J*=7.8, 2H), 7.45 (d, *J*=7.4, 1H), 7.21 (td, *J*=14.3, 13.8, 6.4, 5H), 7.04 (dd, *J*=22.2, 7.7, 3H), 2.49 (s, 3H), 1.39 (s, 6H).

7-methoxy-9,9-dimethyl-N-(4-(methylthio)phenyl)-9H-fluoren-2-amine ***(5)***: Compound 1 (3.02 g, 10 mmol), 4-(Methylthio)aniline (2.09 g, 15 mmol), $Pd_2(dba)_3$ (0.46 g, 0.5 mmol), and NaO*t*-Bu (2.88 g, 30 mmol) were added into 80 mL dry toluene in 250 mL two-necked flask. The mixture was purged with nitrogen for 20 min, then TTBP·HBF_4 (0.29 g, 1 mmol) was further added into the mixture solution, and the reaction was stirred at 110 ℃ for 12 h. After reaction, cool the solution to

room temperature, it was then extracted with dichloromethane, the two phases were separated, and the water phase was extracted twice with dichloromethane. The combined organic extracts were washed three times with water, dried over Na_2SO_4, evaporated, purified with column chromatography (eluting with petroleum ether / dichloromethane, 3/1 v/v) and dried under vacuum to obtain the compound ***5*** as a light-yellow power (2.87 g, 7.96 mmol, 79.6% yield). ^{1}H NMR (400 MHz, DMSO-d_6) δ = 8.25 (s, 1H), 7.53 (dd, *J*=8.3, 2.1, 2H), 7.23 – 7.13 (m, 3H), 7.10 – 6.97 (m, 4H), 6.83 (dd, *J*=8.3, 2.4, 1H), 3.78 (s, 3H), 1.38 (s, 6H).

*N-(4-methoxyphenyl)-9,9-dimethyl-7-(methylthio)-9H-fluoren-2-amine (**6**)*: Compound 2 (3.18 g, 10 mmol), 4-Methoxyaniline (1.85 g, 15 mmol), $Pd_2(dba)_3$ (0.46 g, 0.5 mmol), and NaO*t*-Bu (2.88 g, 30 mmol) were added into 80 mL dry toluene in 250 mL two-necked flask. The mixture was purged with nitrogen for 20 min, then TTBP·HBF_4 (0.29 g, 1 mmol) was further added into the mixture solution, and the reaction was stirred at 110 ℃ for 12 h. After reaction, cool the solution to room temperature, it was then extracted with dichloromethane, the two phases were separated, and the water phase was extracted twice with dichloromethane. The combined organic extracts were washed three times with water, dried over Na_2SO_4, evaporated, purified with column chromatography (eluting with petroleum ether / dichloromethane, 2/1 v/v) and dried under vacuum to obtain the compound ***6*** as a light-yellow power (2.92 g, 8.09 mmol, 80.9% yield). ^{1}H NMR (400 MHz, DMSO-d_6) δ = 8.00 (s, 1H), 7.53 (dd, *J*=8.1, 2.1, 2H), 7.37 (d, *J*=1.9, 1H), 7.15 (dd, *J*=7.9, 1.8, 1H), 7.11 – 7.01 (m, 3H), 6.92 – 6.84 (m, 3H), 3.71 (s, 3H), 1.37 (s, 6H).

*9,9'-([1,1'-biphenyl]-4,4'-diyl)bis(N^3,N^6-bis(9,9-dimethyl-9H-fluoren-2-yl)-N^3,N^6-bis(4-methoxyphenyl)-9H-carbazole-3,6-diamine) (**OP**)*: Compound 3 (2.97 g, 9.42 mmol), Compound 7 (1.50 g, 1.88 mmol), $Pd(OAc)_2$ (0.21 g, 0.94 mmol), and KO*t*-Bu (2.11 g, 18.8 mmol) were added

into 60 mL dry toluene in 250 mL two-necked flask. The mixture was purged with nitrogen for 20 min, then P(*t*Bu)$_3$ (4.42 mL, 10% in Toluene) was further added into the mixture solution, and the reaction was stirred at 120 ℃ for 36 h. After reaction, cool the solution to room temperature, it was then extracted with dichloromethane, the two phases were separated, and the water phase was extracted twice with dichloromethane. The combined organic extracts were washed three times with water, dried over Na_2SO_4, evaporated, purified with column chromatography (eluting with petroleum ether / dichloromethane, 1/1 v/v) and dried under vacuum to obtain the HTM ***OP*** as a beige power (2.71 g, 1.56 mmol, 82.9% yield). ^{1}H NMR (400 MHz, THF-d_8) δ = 8.19 – 8.00 (m, 4H), 7.91 (d, *J*=2.4, 4H), 7.83 (dd, *J*=8.2, 2.0, 4H), 7.60 (d, *J*=7.9, 4H), 7.55 – 7.43 (m, 8H), 7.37 (d, *J*=7.4, 4H), 7.32 – 7.08 (m, 24H), 6.96 – 6.79 (m, 12H), 3.82 – 3.73 (m, 12H), 1.37 (d, *J*=2.2, 24H). ^{13}C NMR (101 MHz, THF-d_8) δ = 155.9, 154.7, 153.2, 149.0, 141.7, 141.5, 139.3, 138.0, 137.3, 131.9, 130.6, 128.6, 128.4, 127.0, 126.6, 125.9, 125.6, 125.1, 124.5, 122.0, 120.1, 119.8, 118.7, 114.9, 114.4, 110.5, 67.0, 66.9, 66.8, 66.7, 66.6, 66.6, 66.4, 66.2, 66.0, 64.7, 54.5, 46.4, 30.6, 26.5, 24.9, 24.7, 24.7, 24.5, 24.5, 24.3, 24.1, 23.9, 19.1, 13.1. HRMS-EIS (*m/z*): $[M + H]^+$ cacld for ($C_{124}H_{100}N_6O_4$), 1737.7840, found: 1737.7960.

*9,9'-([1,1'-biphenyl]-4,4'-diyl)bis(N^3,N^6-bis(9,9-dimethyl-9H-fluoren-2-yl)-N^3,N^6-bis(4-(methylthio)phenyl)-9H-carbazole-3,6-diamine) (**SP**)*: Compound 4 (5.94 g, 18.85 mmol), Compound 7 (3.00 g, 3.77 mmol), $Pd(OAc)_2$ (0.42 g, 1.89 mmol), and KO*t*-Bu (4.23 g, 37.7 mmol) were added into 100 mL dry toluene in 250 mL two-necked flask. The mixture was purged with nitrogen for 20 min, then P(*t*Bu)$_3$ (8.86 mL, 10% in Toluene) was further added into the mixture solution, and the reaction was stirred at 120 ℃ for 36 h. After reaction, cool the solution to room temperature, it was then extracted with dichloromethane, the two phases were separated, and the water

phase was extracted twice with dichloromethane. The combined organic extracts were washed three times with water, dried over Na_2SO_4, evaporated, purified with column chromatography (eluting with petroleum ether / dichloromethane, 1/1 v/v) and dried under vacuum to obtain the HTM ***SP*** as a beige power (5.11 g, 2.84 mmol, 75.2% yield). ^{1}H NMR (400 MHz, THF-d_8) δ = 8.10 (d, *J*=8.1, 4H), 7.98 (d, *J*=2.6, 4H), 7.87 – 7.82 (m, 4H), 7.64 (d, *J*=7.5, 4H), 7.58 (d, *J*=8.3, 4H), 7.52 (d, *J*=8.8, 4H), 7.39 (d, *J*=7.4, 4H), 7.32 – 7.22 (m, 14H), 7.21 – 7.16 (m, 10H), 7.07 (d, *J*=8.2, 8H), 7.00 (d, *J*=8.1, 4H), 2.44 (d, *J*=1.9, 12H), 1.39 (s, 24H). ^{13}C NMR (101 MHz, THF-d_8) δ = 154.8, 153.3, 148.0, 146.6, 140.9, 139.1, 138.4, 133.3, 130.7, 128.5, 128.4, 127.1, 126.7, 126.0, 125.7, 124.5, 123.2, 122.1, 121.6, 120.3, 118.9, 118.6, 116.8, 110.7, 67.0, 66.9, 66.8, 66.7, 66.6, 66.6, 66.4, 66.2, 66.0, 46.5, 26.4, 24.9, 24.7, 24.7, 24.5, 24.5, 24.4, 24.3, 24.1, 23.9, 15.8. HRMS-EIS (*m/z*): $[M + H]^+$ cacld for ($C_{124}H_{100}N_6S_4$), 1801.6926, found: 1801.7030.

*9,9'-([1,1'-biphenyl]-4,4'-diyl)bis(N^3,N^6-bis(7-methoxy-9,9-dimethyl-9H-fluoren-2-yl)-N^3,N^6-bis(4-(methylthio)phenyl)-9H-carbazole-3,6-diamine) (**OFSP**)*: Compound 5 (6.81 g, 18.85 mmol), Compound 7 (3.00 g, 3.77 mmol), $Pd(OAc)_2$ (0.42 g, 1.89 mmol), and KO*t*-Bu (4.23 g, 37.7 mmol) were added into 100 mL dry toluene in 250 mL two-necked flask. The mixture was purged with nitrogen for 20 min, then P(*t*Bu)$_3$ (8.86 mL, 10% in Toluene) was further added into the mixture solution, and the reaction was stirred at 120 ℃ for 36 h. After reaction, cool the solution to room temperature, it was then extracted with dichloromethane, the two phases were separated, and the water phase was extracted twice with dichloromethane. The combined organic extracts were washed three times with water, dried over Na_2SO_4, evaporated, purified with column chromatography (eluting with petroleum ether / dichloromethane, 2/3 v/v) and dried under vacuum to obtain the HTM ***OFSP*** as a light-yellow power (5.63 g, 2.93 mmol, 77.8% yield). ^{1}H NMR (400 MHz, THF-d_8) δ = 8.09 (d,

J=7.9, 4H), 7.97 (s, 4H), 7.84 (d, *J*=8.0, 4H), 7.57 – 7.46 (m, 12H), 7.31 – 7.23 (m, 8H), 7.21 – 7.13 (m, 8H), 7.09 – 6.95 (m, 16H), 6.85 (d, *J*=8.4, 4H), 3.83 (t, *J*=1.6, 12H), 2.43 (t, *J*=1.6, 12H), 1.38 (d, *J*=2.3, 24H). ^{13}C NMR (101 MHz, THF-d_8) δ = 159.4, 155.2, 154.4, 146.9, 141.0, 138.3, 137.2, 133.7, 131.8, 130.2, 128.5, 128.4, 124.5, 122.7, 122.1, 119.7, 119.4, 117.3, 112.3, 108.3, 67.0, 66.9, 66.8, 66.6, 66.6, 66.4, 66.2, 66.0, 54.5, 46.5, 26.5, 24.9, 24.7, 24.7, 24.5, 24.5, 24.4, 24.3, 24.1, 23.9, 15.9. HRMS-EIS (*m/z*): $[M + H]^+$ cacld for ($C_{128}H_{108}N_6O_4S_4$), 1921.7348, found: 1921.7476.

*9,9'-([1,1'-biphenyl]-4,4'-diyl)bis(N^3,N^6-bis(9,9-dimethyl-7-(methylthio)-9H-fluoren-2-yl)-N^3,N^6-bis(4-methoxyphenyl)-9H-carbazole-3,6-diamine) (**OPSF**)*: Compound 6 (6.81 g, 18.85 mmol), Compound 7 (3.00 g, 3.77 mmol), $Pd(OAc)_2$ (0.42 g, 1.89 mmol), and KO*t*-Bu (4.23 g, 37.7 mmol) were added into 100 mL dry toluene in 250 mL two-necked flask. The mixture was purged with nitrogen for 20 min, then P(*t*Bu)$_3$ (8.86 mL, 10% in Toluene) was further added into the mixture solution, and the reaction was stirred at 120 ℃ for 36 h. After reaction, cool the solution to room temperature, it was then extracted with dichloromethane, the two phases were separated, and the water phase was extracted twice with dichloromethane. The combined organic extracts were washed three times with water, dried over Na_2SO_4, evaporated, purified with column chromatography (eluting with petroleum ether / dichloromethane, 2/3 v/v) and dried under vacuum to obtain the HTM ***OPSF*** as a light-yellow power (5.89 g, 3.07 mmol, 81.4% yield). ^{1}H NMR (400 MHz, THF-d_8) δ = 8.13 – 8.04 (m, 4H), 7.91 (d, *J*=2.5, 4H), 7.83 (d, *J*=8.1, 4H), 7.56 – 7.45 (m, 12H), 7.33 (s, 4H), 7.28 (d, *J*=8.7, 4H), 7.22 – 7.09 (m, 16H), 6.93 – 6.82 (m, 12H), 3.82 – 3.73 (m, 12H), 2.51 (t, *J*=1.5, 12H), 1.37 (d, *J*=2.3, 24H). ^{13}C NMR (101 MHz, THF-d_8) δ = 155.9, 154.5, 154.0, 148.9, 141.6, 141.5, 138.0, 137.3, 136.8, 136.0, 131.5, 128.4, 127.0, 125.9, 125.6, 125.1, 124.5, 121.1, 120.0, 119.8, 119.1, 117.7, 114.9, 114.4, 110.5, 67.0, 66.9, 66.8, 66.6, 66.6, 66.4, 66.2, 66.0, 54.6, 46.4, 26.4, 24.9, 24.7, 24.7, 24.5,

24.5, 24.3, 24.1, 23.9, 15.4. HRMS-EIS (*m/z*): $[M + H]^+$ cacld for ($C_{128}H_{108}N_6O_4S_4$), 1921.7348, found: 1921.7352.

2. Device fabrication.

2.1 Materials and Solvents.

FTO conductive glass, $MAPbBr_3$, BAI, PbI_2 and Spiro-OMeTAD were purchased from Advanced Electron Technology Co., Ltd. (China). $HC(NH_2)_2I$ (FAI) and CH_3NH_3Cl (MACl) were received from Greatcell. Dimethylformamide (DMF), chlorobenzene (CB) and dimethyl sulfoxide (DMSO) were bought from Sigma-Aldrich. 4-tert-butylpyridine (TBP), and lithium bis(trifluoromethylsulfonyl)imide (Li-TFSI) and tris(2-(1*H*-pyrazol-1-yl)-4-tert-butylpyridine)-cobalt (III) (FK209) were bought from Xi'An P-OLED Co. (China). The SnO_2 colloid precursor was obtained from Alfa Aesar (tin (IV) oxide, 15% in H_2O colloidal dispersion). The titanium diisopropoxide bis(acetylacetonate) (75 wt% in isopropanol) was purchased from TCI.

2.2 Details.

Planar n-i-p PSCs were fabricated with a configuration of FTO/c-TiO_2/SnO_2/ $(FAPbI_3)_{0.992}(MAPbBr_3)_{0.008}$/HTL/Au, where the c-$TiO_2$/$SnO_2$ as the electron transport layer (ETL), the perovskite $(FAPbI_3)_{0.992}(MAPbBr_3)_{0.008}$ as the light absorber layer, the doped Spiro-OMeTAD and studied HTM as the hole transport layer (HTL), the gold as the anode.

(1) Preparation of the FTO conductive glass

FTO conductive glass was cleaned by sequentially washing with detergent, deionized water, acetone, and ethyl alcohol and then dried under a nitrogen atmosphere. The substrates were treated with oxygen plasma for 20 min.

(2) Fabrication of the ETL.

Compact TiO_2 (c-TiO_2) layer was deposited on top of the FTO conductive glass using the spray pyrolysis method (O_2 as the carrier gas) and the substrate was preheated to 450 °C. A c-TiO_2 precursor solution was prepared by diluting 0.6 mL titanium diisopropoxide bis(acetylacetonate) (75 wt% in isopropanol) in 5.4 mL absolute ethanol. Note that the spraying process must be even and dense. After spray pyrolysis, the FTO/c-TiO_2 substrate was heated at 450 °C for 1 h and then cooled to ambient temperature. The thickness of c-TiO_2 is about 20 nm. The compact SnO_2 layer was fabricated by the PAA modification method. SnO_2 colloid precursor was diluted 25 times with deionized water and then mixed with PAA (1 mg/mL) under stirring at 80 °C for 2 h. The resulting solution was spin coated onto the c-TiO_2 layer at 4000 rpm for 30 s. The substrates were heated at 160 °C for 30 min, followed by spin-coating 10 mM KCl in deionized water at 3000 rpm for 30 s and annealing at 160 °C for 10 min.

(3) Fabrication of the light absorber layer.

Before perovskite deposition, the FTO/ETL substrate was treated with UV-Ozone for 20 min. The perovskite precursor solution was prepared by adding 5.4 mg $MAPbBr_3$, 33.1 mg MACl, 240.8 mg FAI, 716.4 mg PbI_2, in 1 mL DMF and DMSO mixed solvent (8:1, v/v), which was then stirred for 6 h and used the polyvinylidene fluoride (PVDF) membrane with a pore size of 0.22 μm for filtration. The perovskite precursor solution was spin-coated using two steps onto the FTO/ETL substrate at 1000 rpm for 10 s and 6000 rpm for 30 s, and chlorobenzene anti-solvent (100 μL for FTO area of 1.5 cm x 1.5 cm, 180 μL for FTO area of 2 cm x 2 cm) was drop-casted at the end of the spin-coating 10s. The film was annealed at 110 °C for 1 h. After the substrates had cooled to room temperature, BAI/IPA solution (3 mg/mL) was spin-coated on the perovskite layer at 5000 rpm for 30 s for surface passivation.

(4) Fabrication of the HTL.

The Spiro-OMeTAD and studied HTL were spin-coated on the perovskite film at 4000 rpm for 30 s and 3000 rpm for 30 s, respectively. The Spiro-OMeTAD solution (90 mg/mL in CB) was doped with 39 μL TBP, 23 μL Li-TFSI (520 mg/mL in acetonitrile) and 10 μL FK209 (320 mg/mL in acetonitrile). The OP, SP, OFSP and OPSF solution (35 mg/mL in CB) was doped with 28.8 μL tBP, 17.5 μL Li-TFSI (520 mg/mL in acetonitrile).

(5) Fabrication of the anode.

The 100 nm Au electrode was thermally evaporated on top of HTL. To be mentioned, metal masks with an active area of 0.055 and 1 cm^2 were used to determine the effective device area for small-sized and large-sized PSCs, respectively.

3. Characterizations.

3.1 Materials characterizations.

^1H and ^{13}C NMR spectra were recorded on a Bruker AM 400 spectrometer with the chemical shifts against TMS, operating at 400 and 101 MHz, respectively. High resolution mass spectrometry (HRMS) results were obtained with a Thermo Scientific Combined Quadrupole Mass Spectrometer.

3.2 Device characterizations.

Light source for the photocurrent-voltage (*J–V*) measurement is an AM 1.5G solar simulator (Newport ORIEL Sol3A). The incident light intensity was 100 $mW \cdot cm^{-2}$ calibrated with a standard Si solar cell. The tested solar cells were masked to a working area of 0.055 and 1cm^2. The photocurrent-voltage (*J–V*) curves were obtained by the linear sweep voltammetry (LSV) method using a Keithley 2400 source-measure unit. The measurement of the incident-photon-to-current conversion efficiency (IPCE) was performed with CEL-QPCE3000 photoelectric chemical quantum

efficiency testing and analysis system. The scanning electron microscope (SEM) images were taken on a JEOL JSM-7800. The electrochemical impedance spectroscopy (EIS) was performed using a two electrode system under dark condition with electrochemical workstation (Zahner PP211). The EIS spectra were recorded in the frequency from 100 mHz to 1 MHz with a bias voltage of 1.20 V.

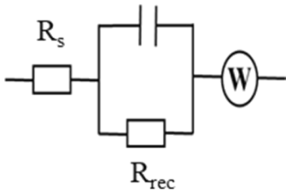

4. Theoretical calculations

Geometrical optimization and quantum chemical calculations of the hole recombination energy at the B3LYP/6-31(d) level were performed using the DFT method. All calculations are carried out with the Gaussian 09 package.[3]

The reorganization energy, is determined by four energies, (the Nelson four-point method)[4]:

$$\lambda = E_+^* - E_+ + E^* - E$$

Where the is the energy of the neutral molecule in the cation symmetry, and the E^* is the energy of the cationic molecule in the neutral symmetry; the E^+ and are the optimized energies of the cationic and neutral molecules.

5. Figures.

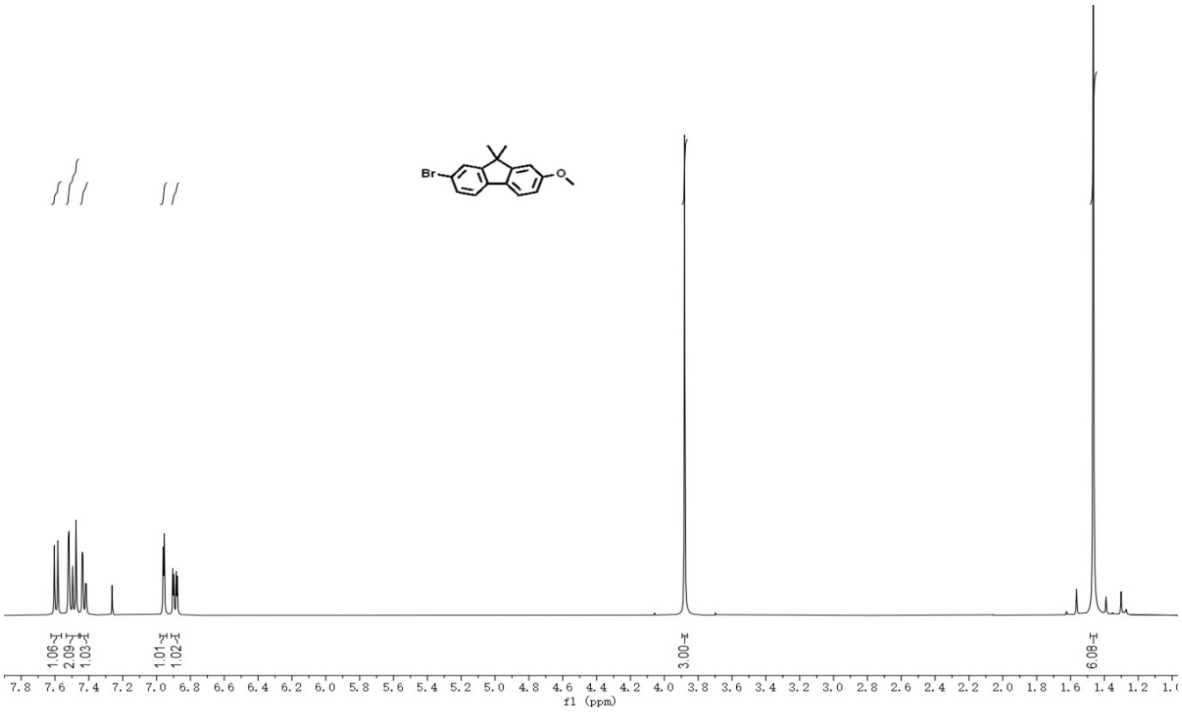

Figure S1. ^{1}H-NMR spectrum of the studied compound 1.

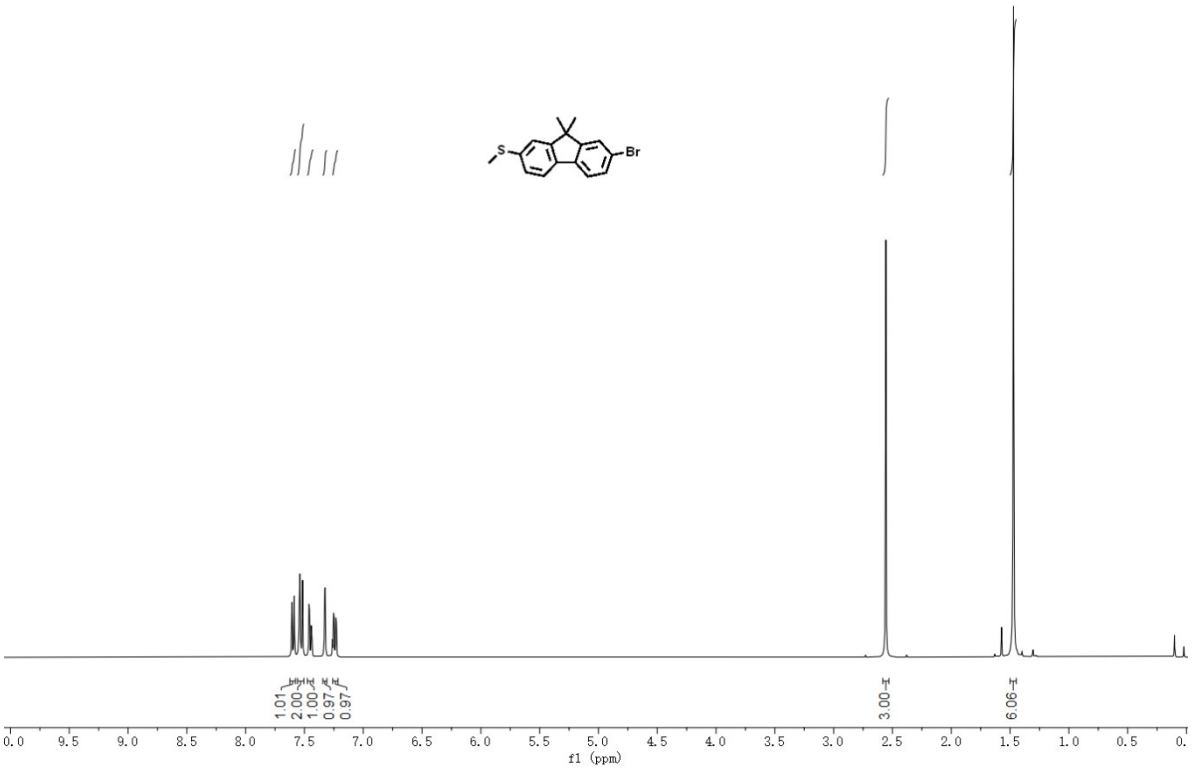

Figure S2. ^{1}H-NMR spectrum of the studied compound 2.

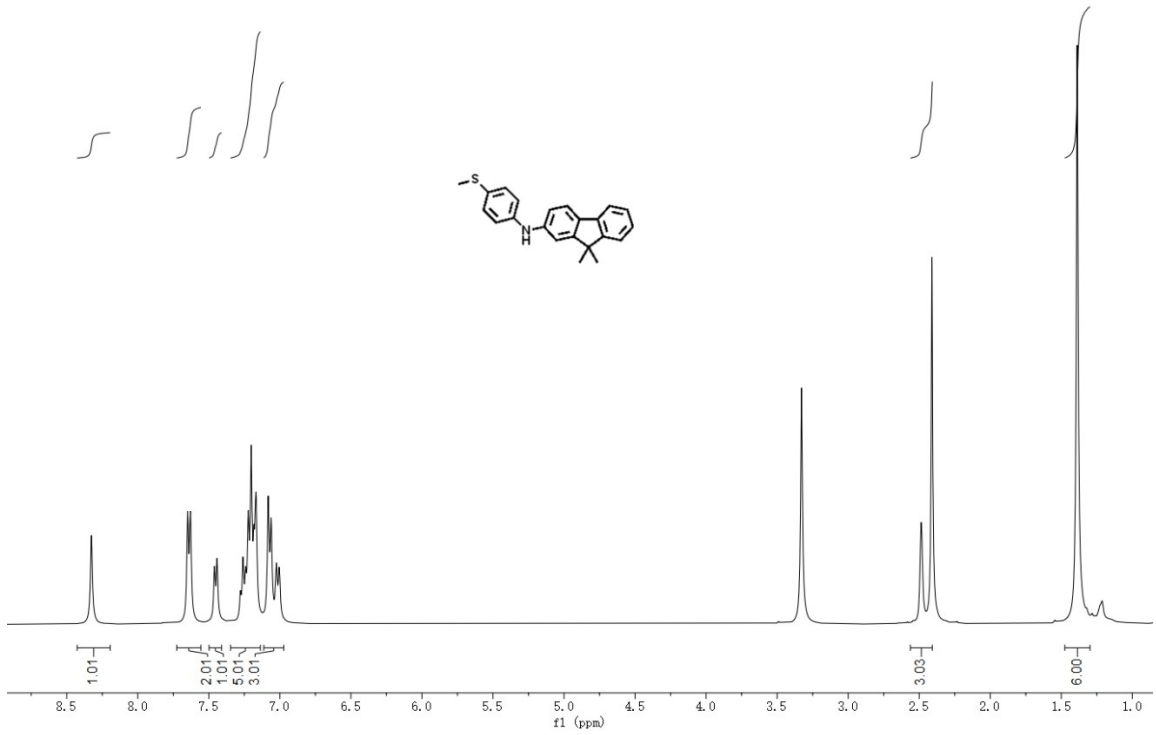

Figure S3. ^{1}H-NMR spectrum of the studied compound 4.

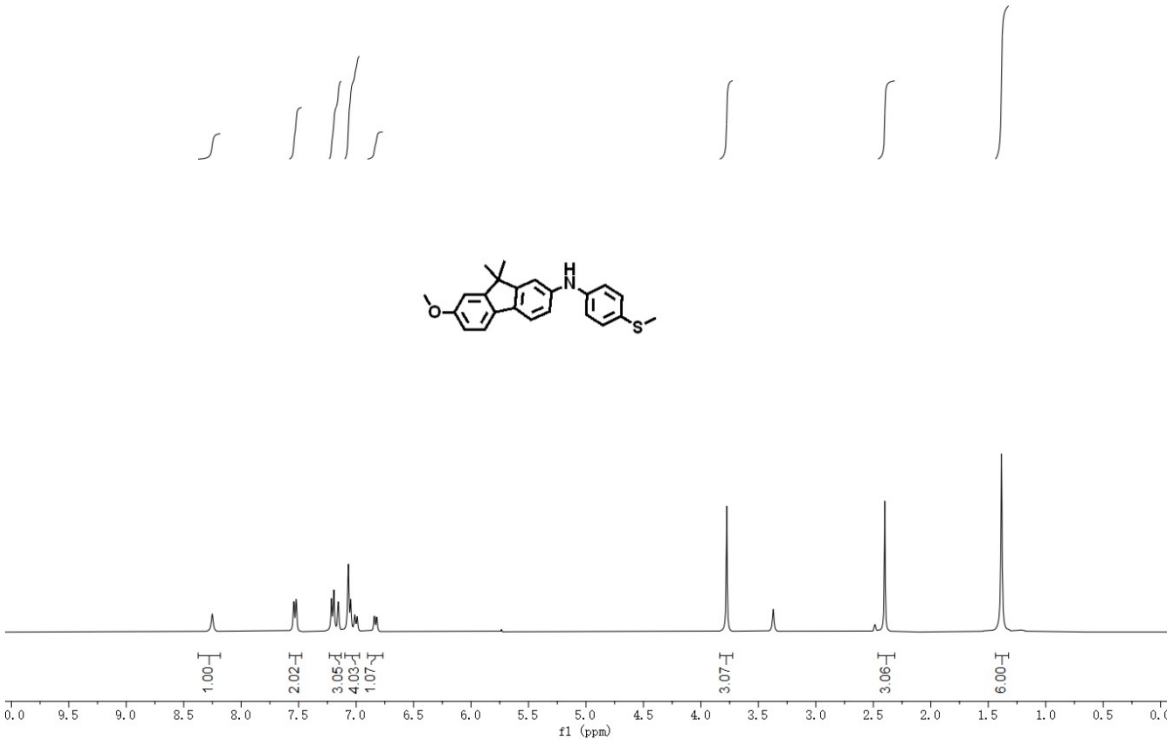

Figure S4. ^{1}H-NMR spectrum of the studied compound 5.

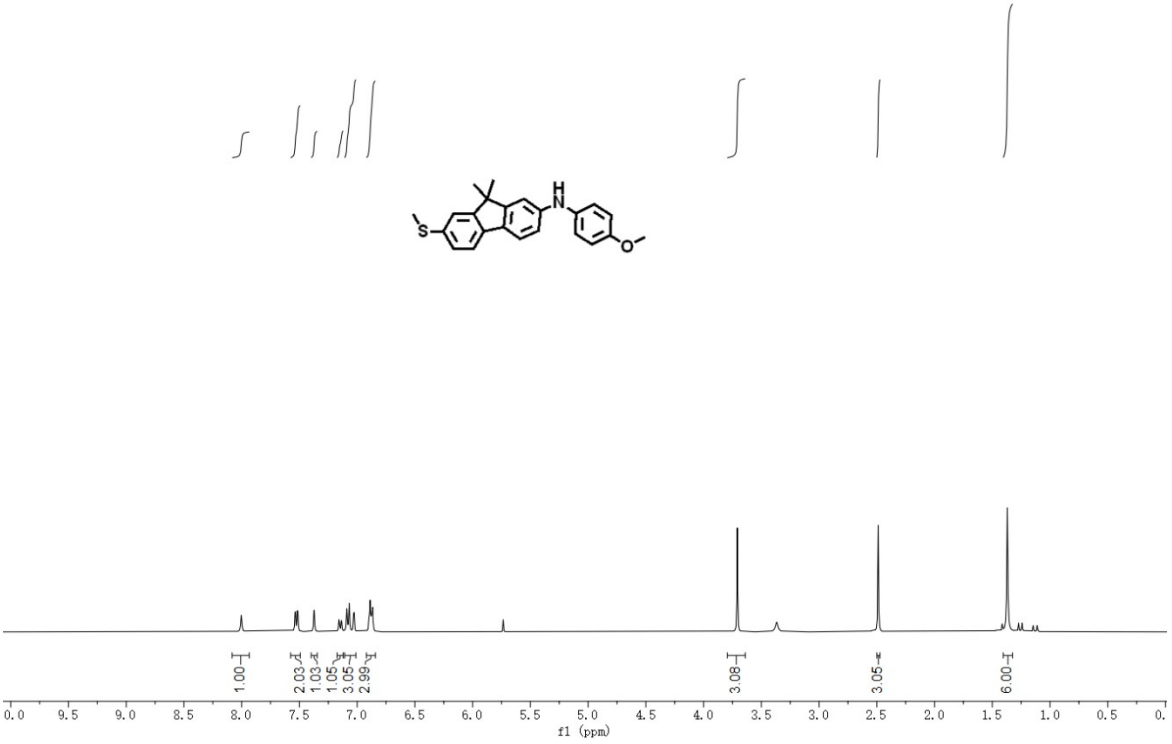

Figure S5. ^{1}H-NMR spectrum of the studied compound 6.

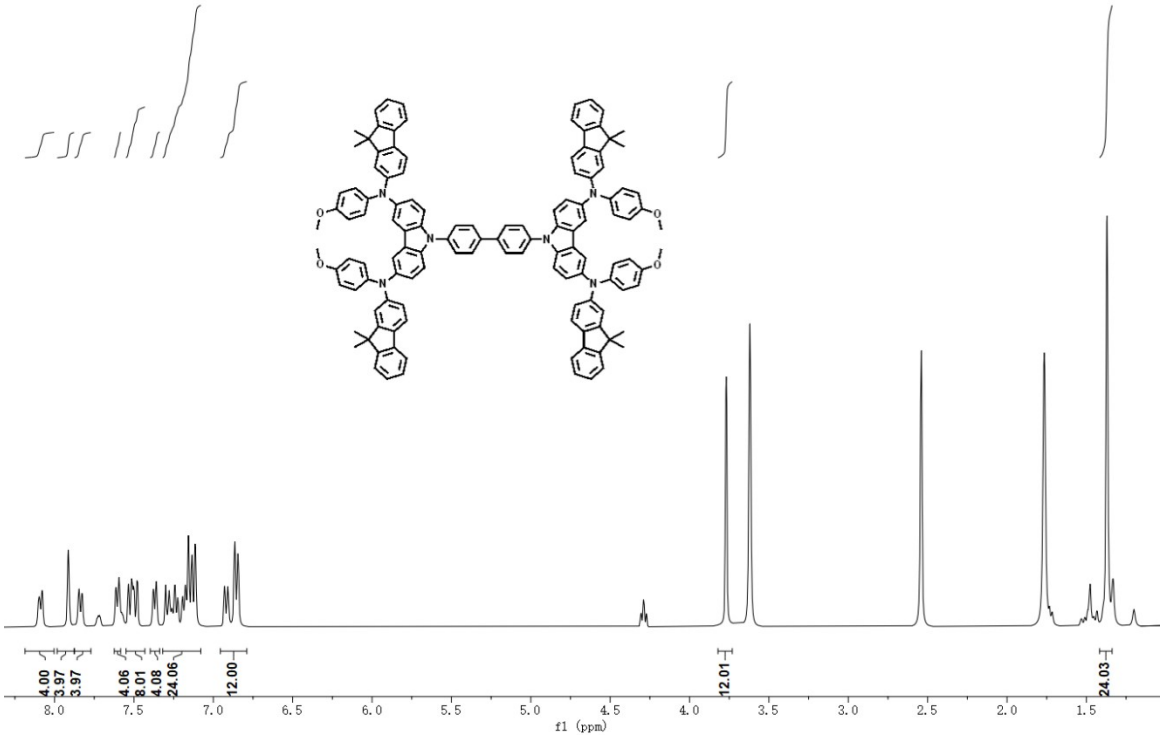

Figure S6. ^{1}H-NMR spectrum of the studied HTM **OP**.

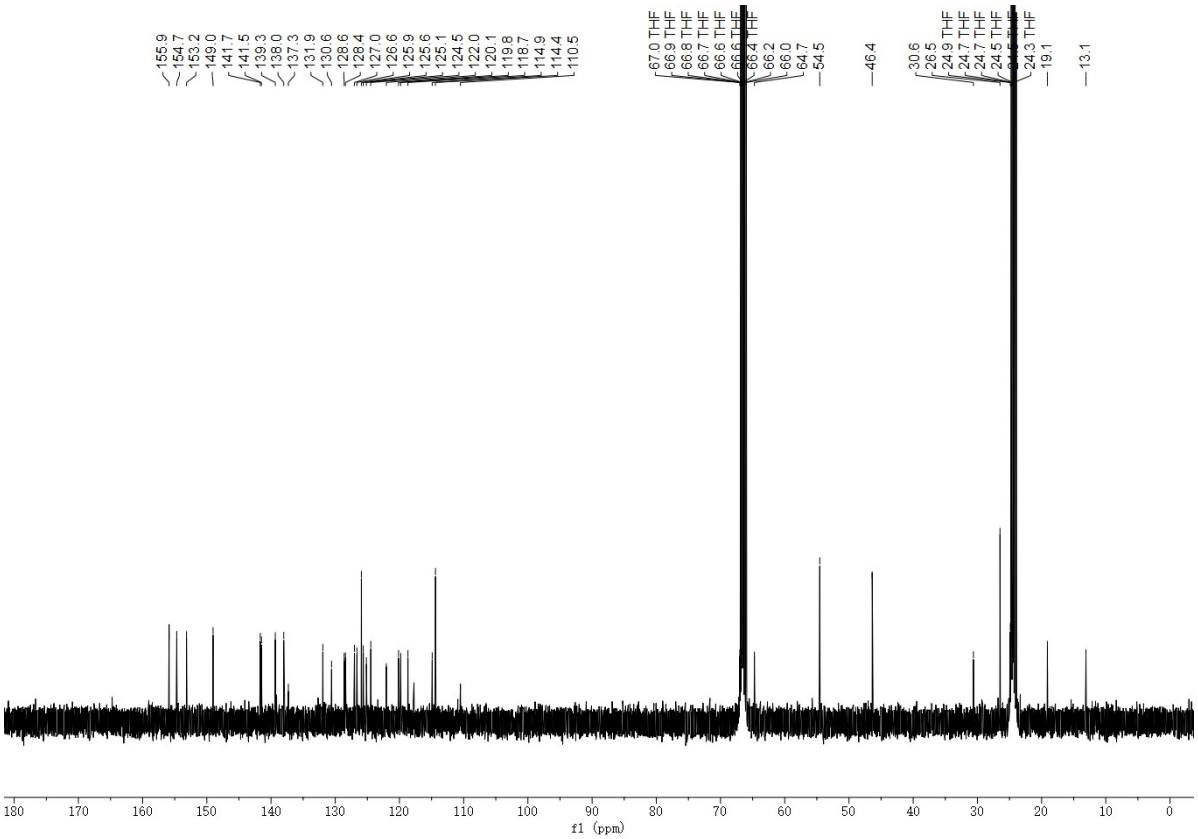

Figure S7. ^{13}C-NMR spectrum of the studied HTM **OP**.

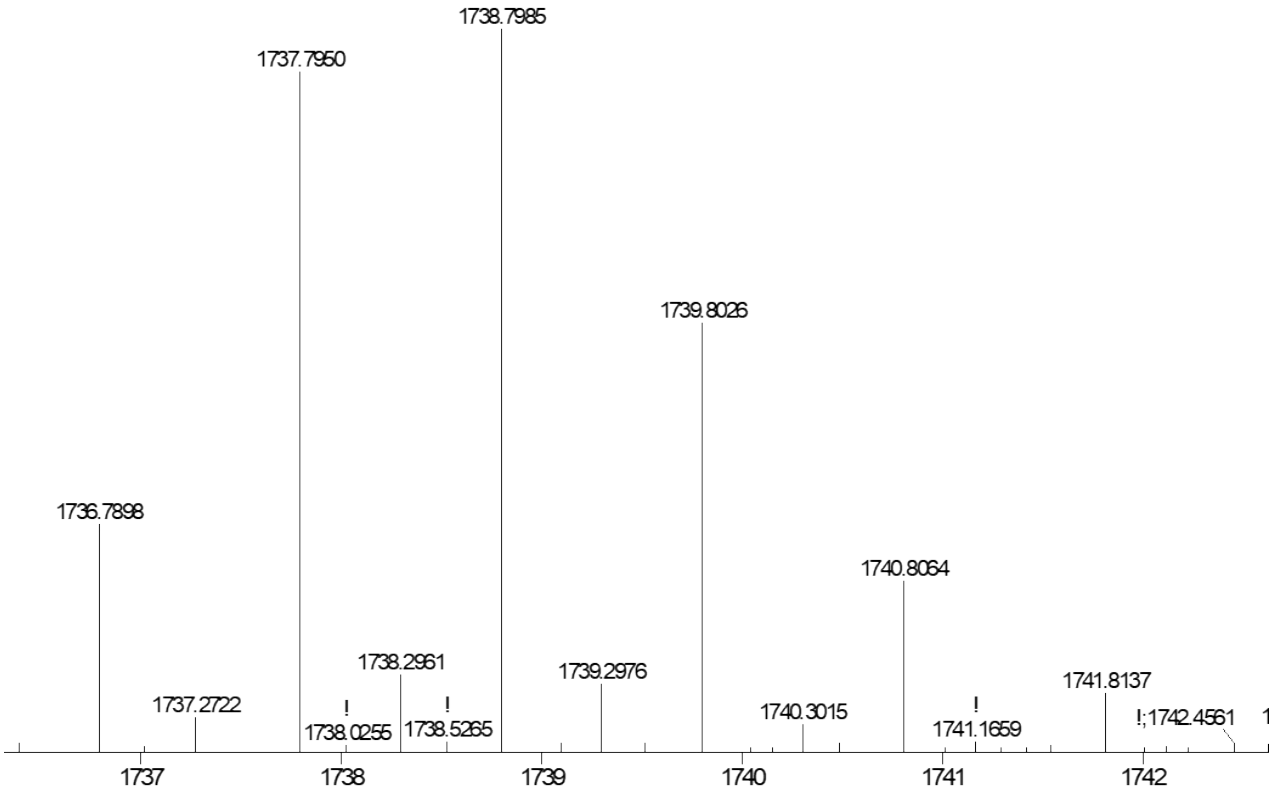

Figure S8. HRMS spectrum of the studied HTM **OP**.

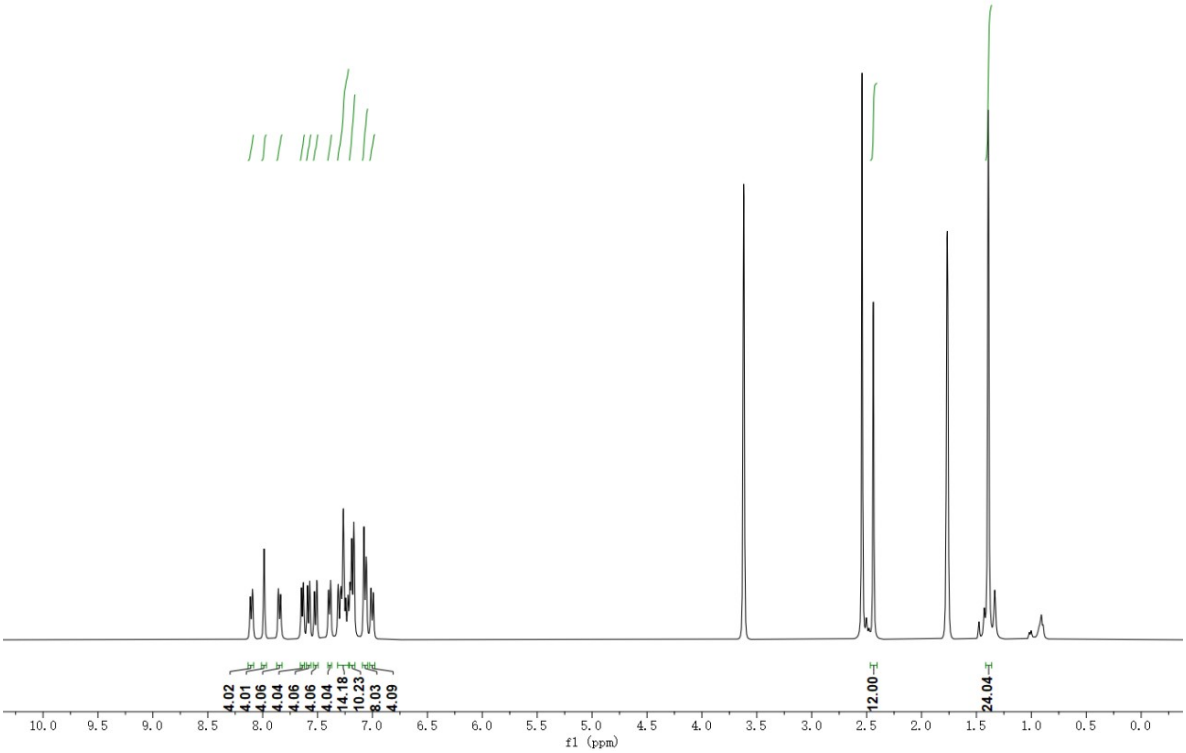

Figure S9. ^{1}H-NMR spectrum of the studied HTM **SP**.

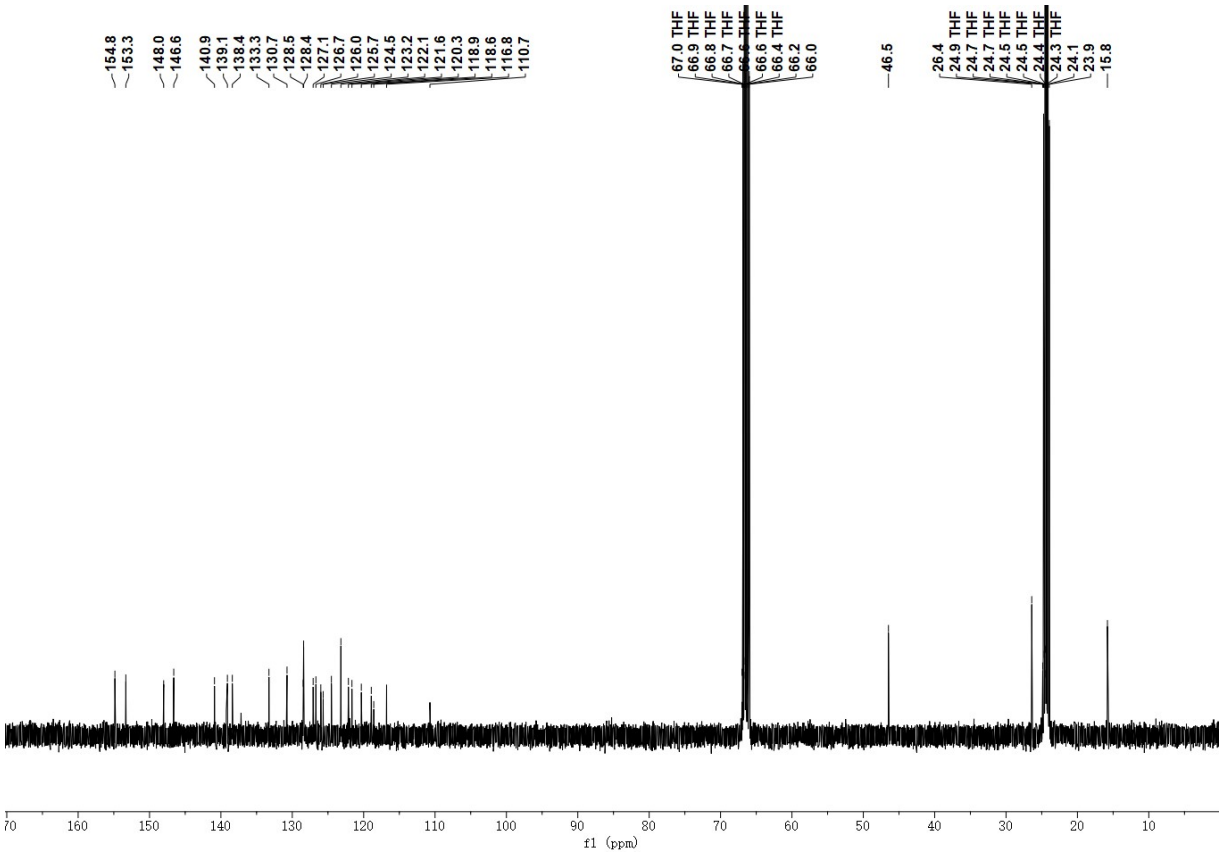

Figure S10. ^{13}C-NMR spectrum of the studied HTM **SP**.

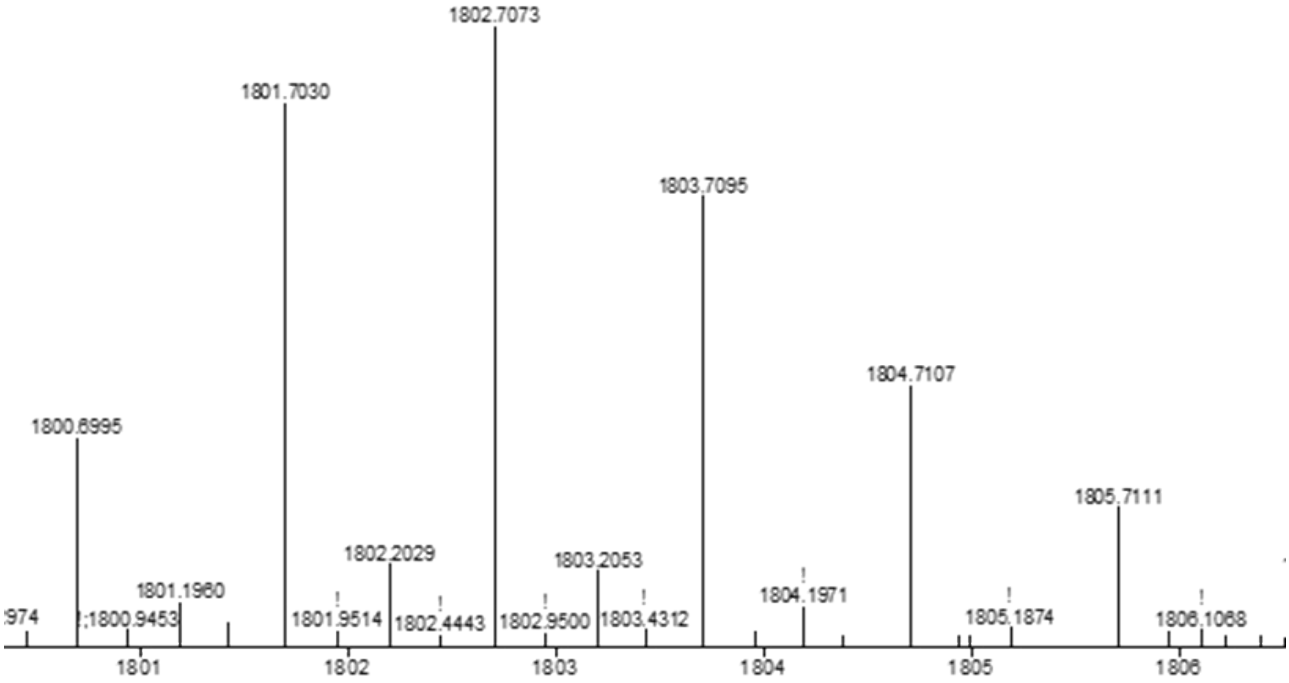

Figure S11. HRMS spectrum of the studied HTM **SP**.

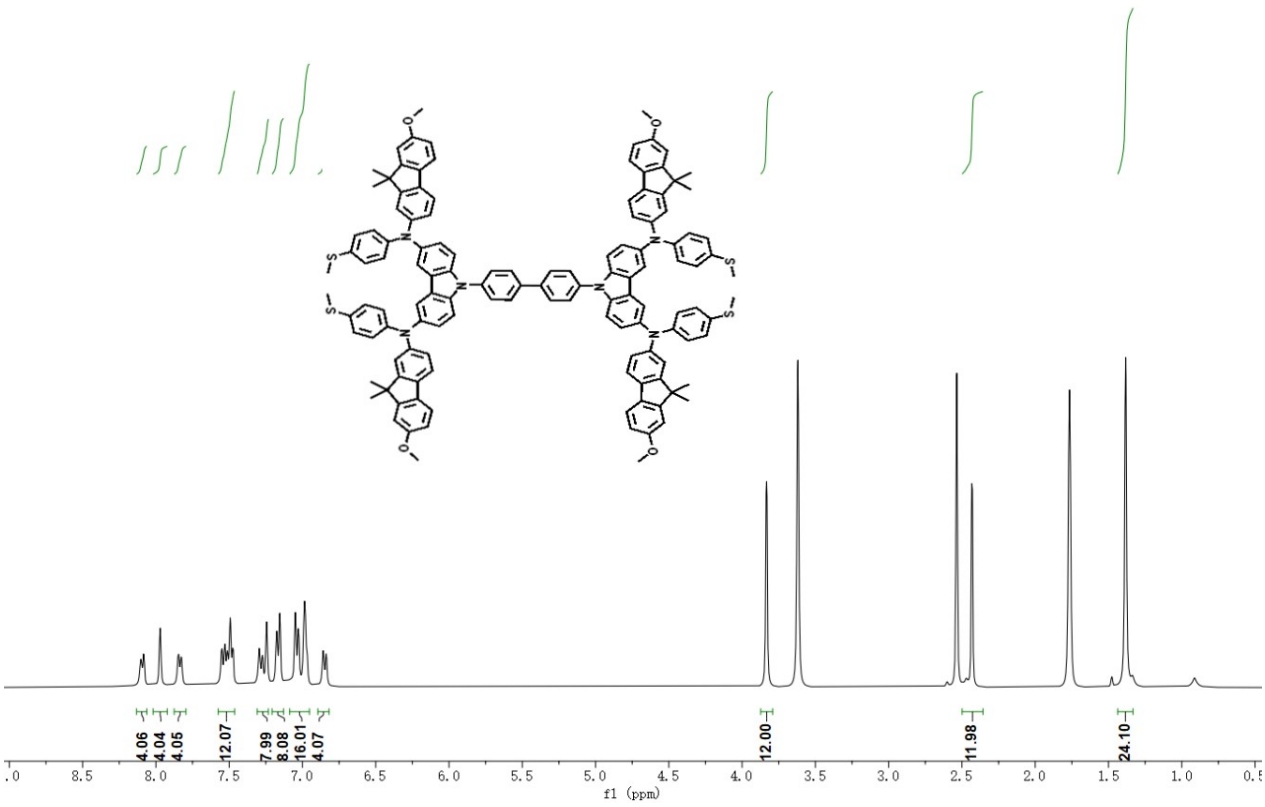

Figure S12. ^{1}H-NMR spectrum of the studied HTM **OFSP**.

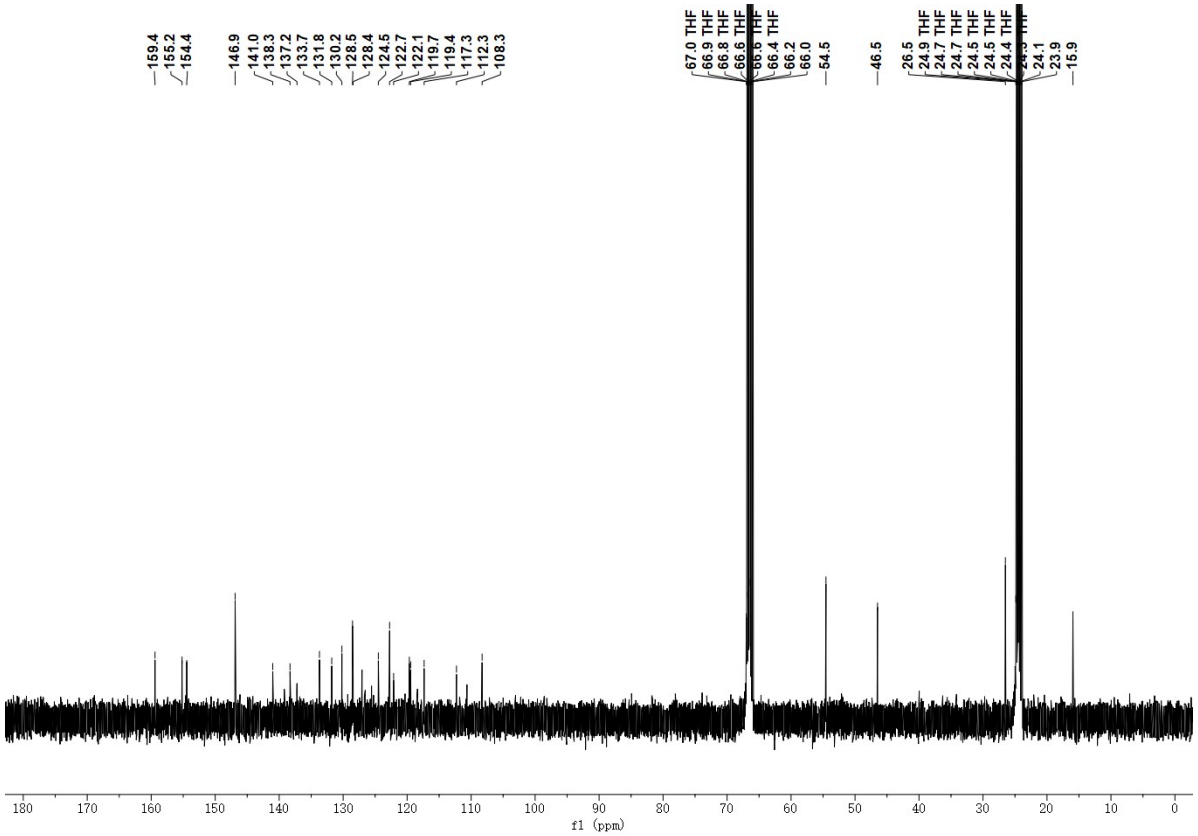

Figure S13. ^{13}C-NMR spectrum of the studied HTM **OFSP**.

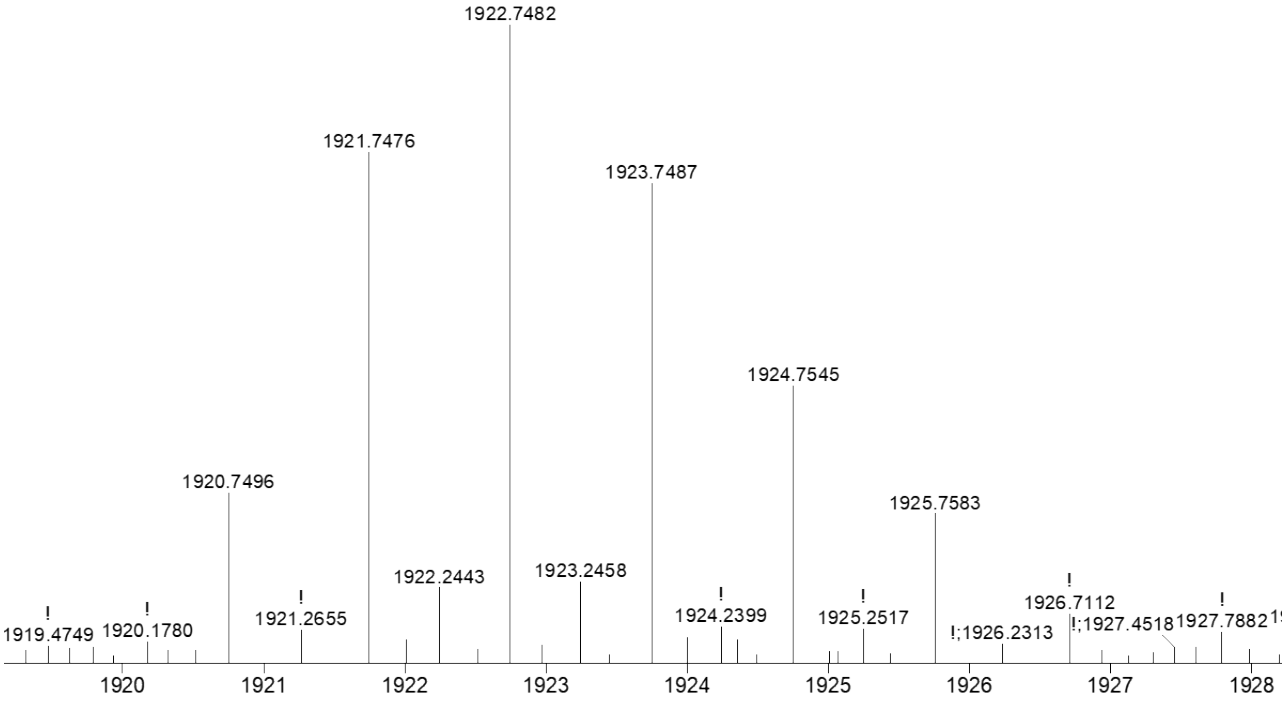

Figure S14. HRMS spectrum of the studied HTM **OFSP**.

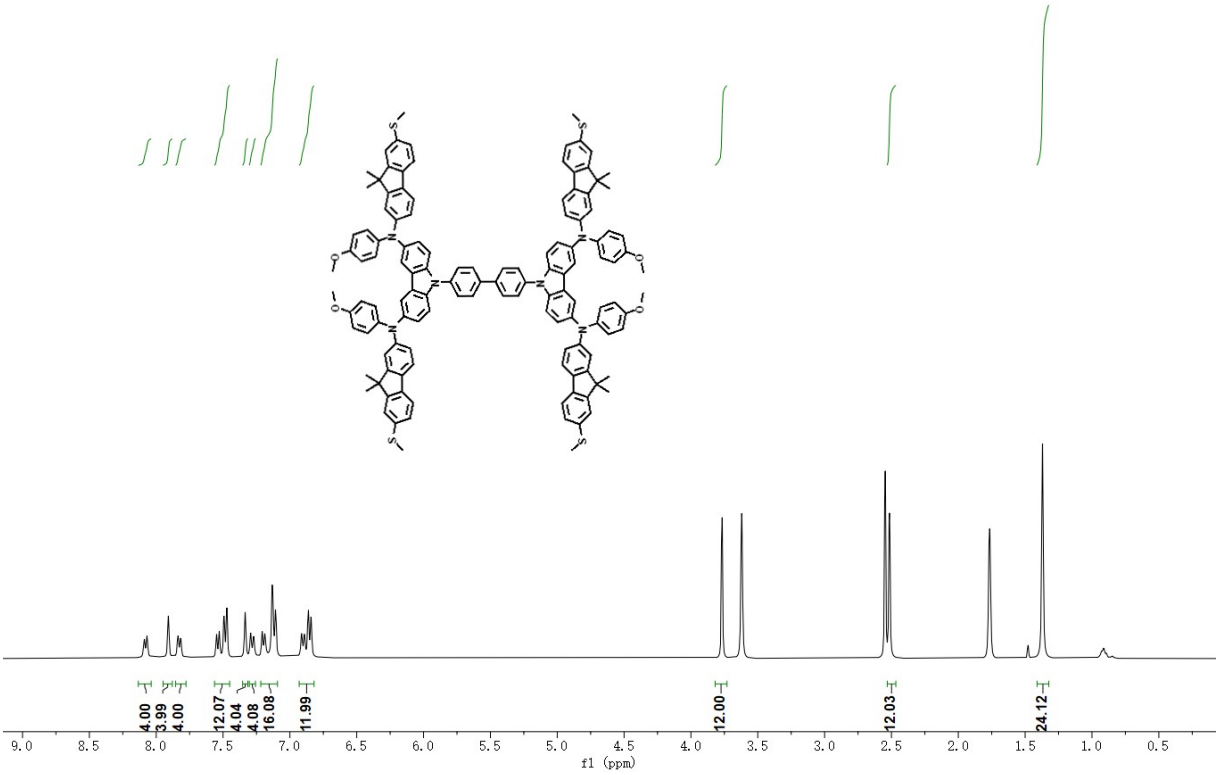

Figure S15. ^{1}H-NMR spectrum of the studied HTM **OPSF**.

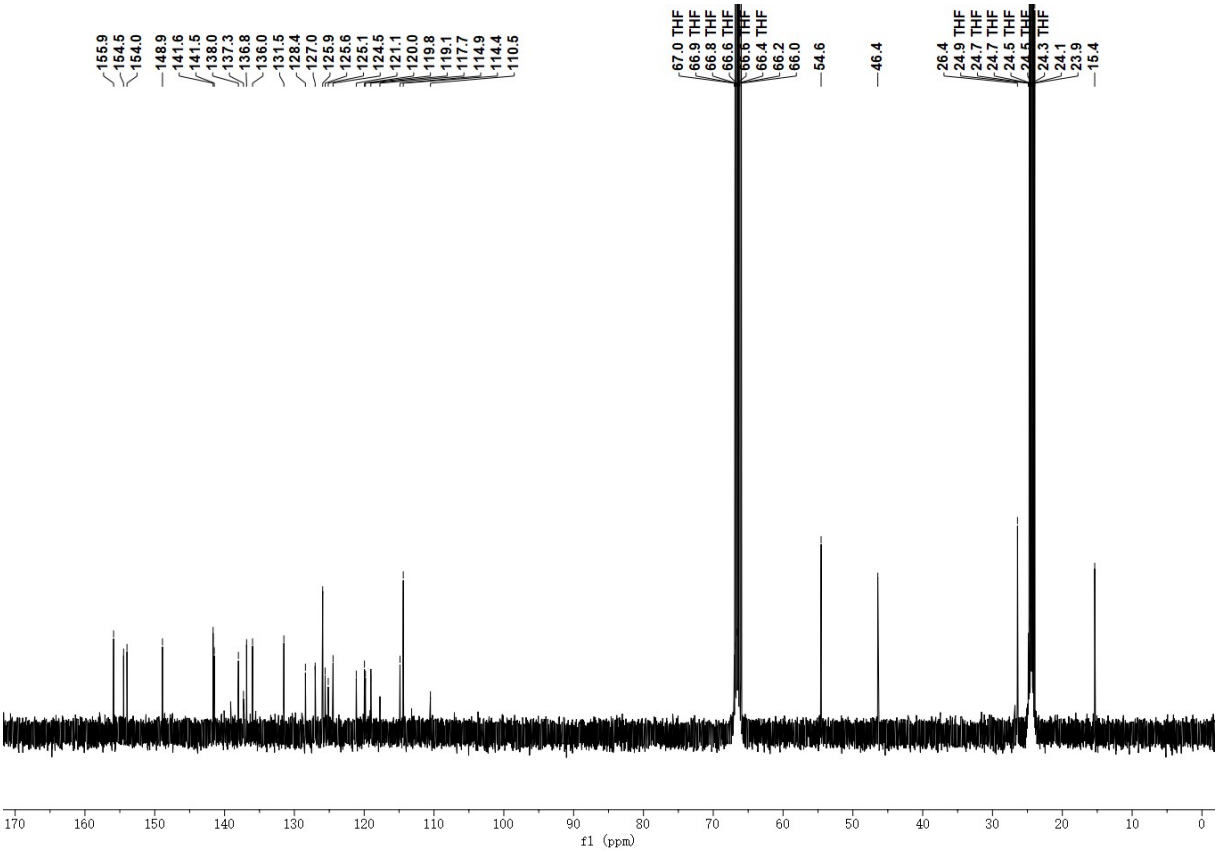

Figure S16. ^{13}C-NMR spectrum of the studied HTM **OPSF**.

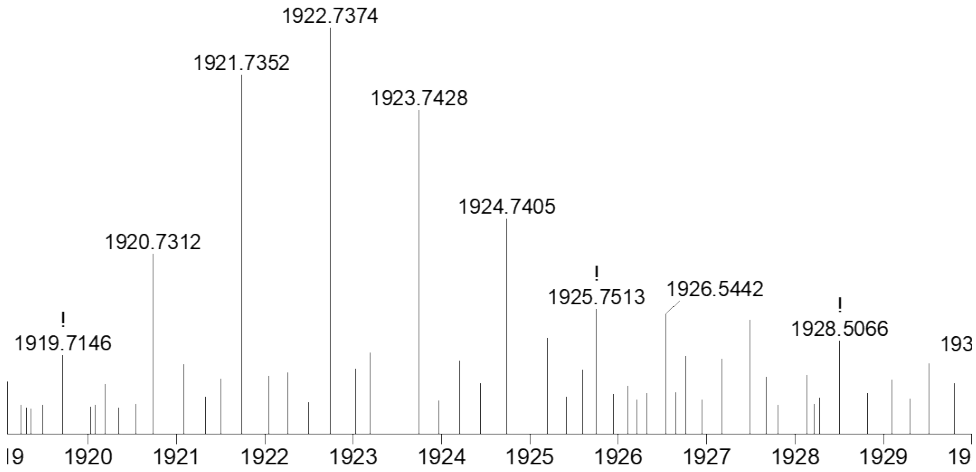

Figure S17. HRMS spectrum of the studied HTM **OPSF**.

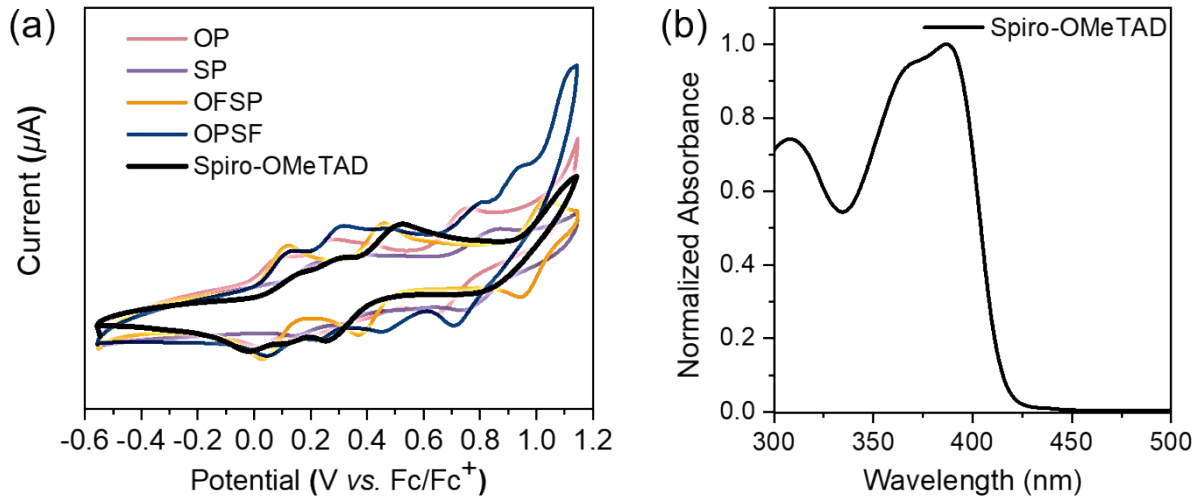

Figure S18. a) Cyclic voltammetry (CV) measurements of Spiro-OMeTAD, OP, SP, OFSP and OPSF in dilute CH_2Cl_2 solution. b) UV-vis absorption spectra of the Spiro-OMeTAD in dilute CH_2Cl_2 solution.

Cyclic voltammetry (CV) was performed in dichloromethane with 0.1 M $TBAPF_6$ as the supporting electrolyte at room temperature. The $Ag/AgNO_3$ electrode, platinum wire, and glassy carbon electrode were used as the reference electrode, counter electrode, and working electrode, respectively. The $Ag/AgNO_3$ reference electrode was calibrated using a ferrocene/ferrocenium (Fc/Fc^+) redox couple as an external standard whose oxidation potential is –5.1 eV with respect to the vacuum level.

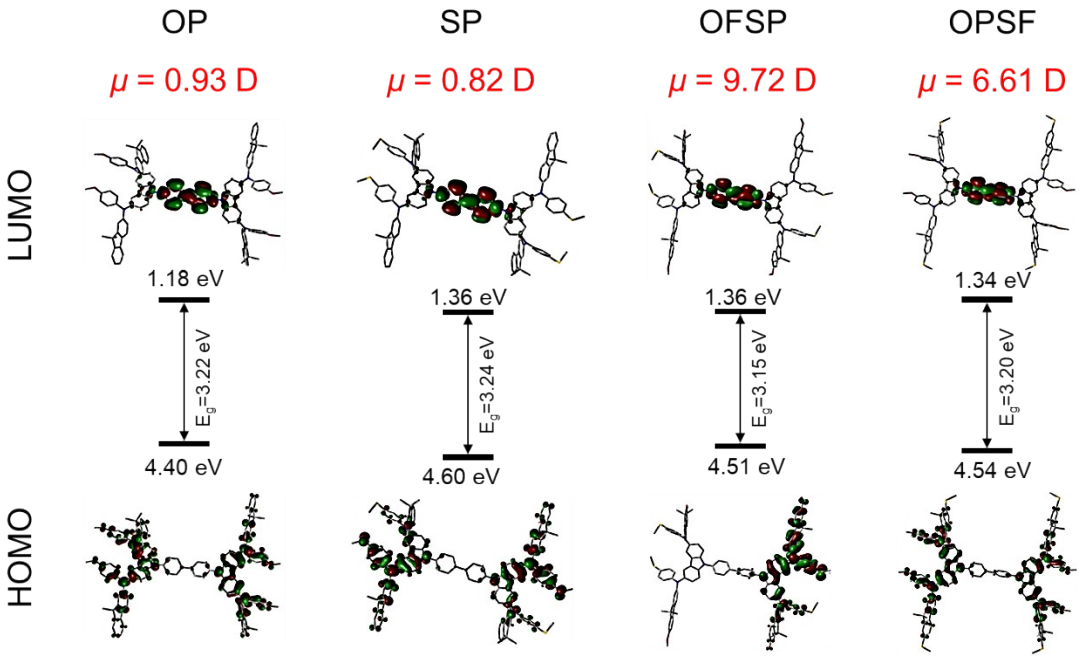

Figure S19. The HOMO/LUMO distribution of OP, SP, OFSP and OPSF including their calculated dipole moments (μ).

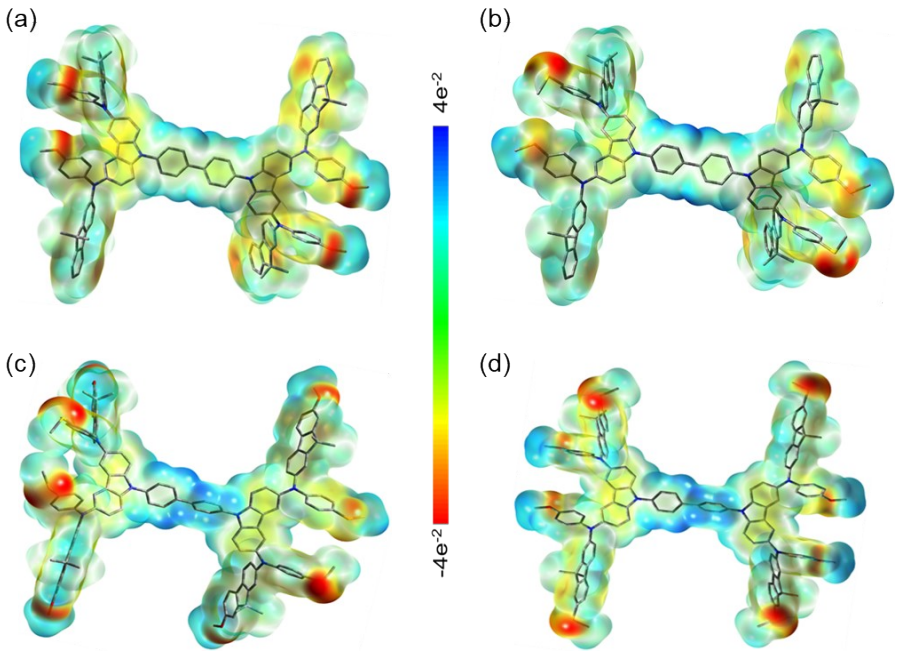

Figure S20. The electrostatic surface potential (ESP) for OP, SP, OFSP and OPSF.

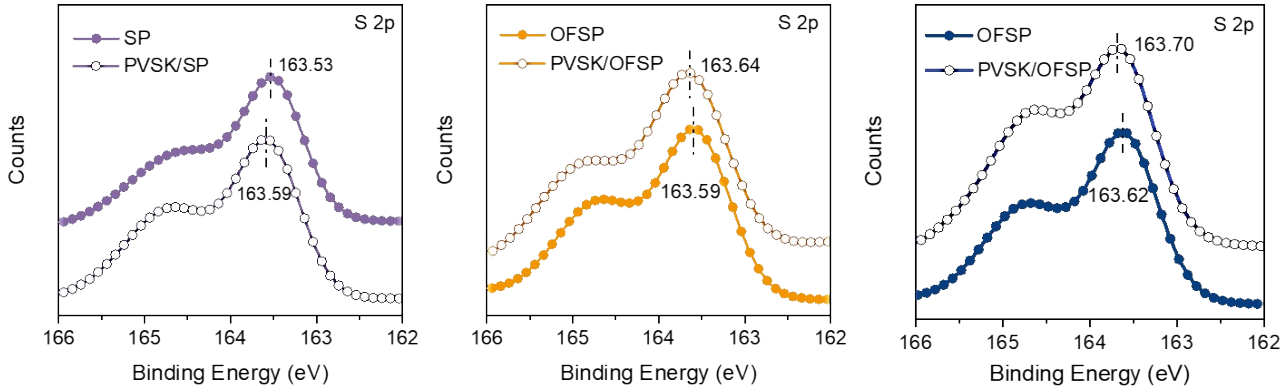

Figure S21. XPS spectra (S 2p) of the HTMs and perovskite films coated with different HTMs.

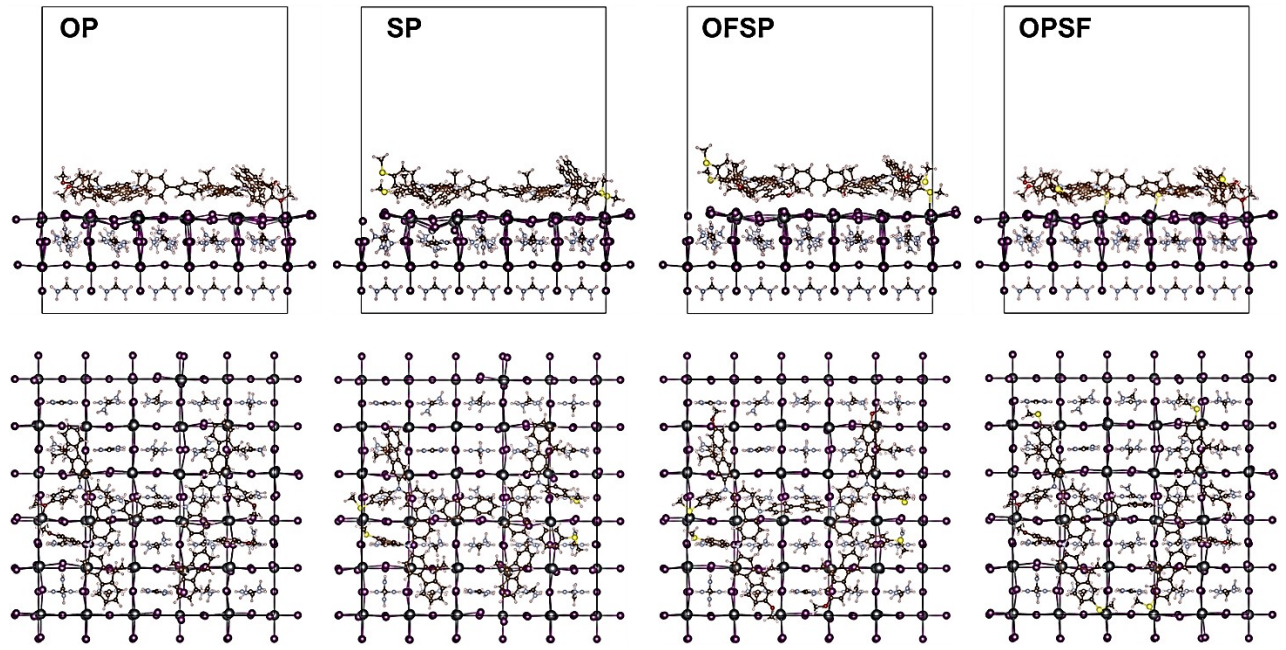

Figure S22. Top views and Side views of OP, SP, OFSP and OPSF adsorbed on a PbI_2-terminal perovskite surface.

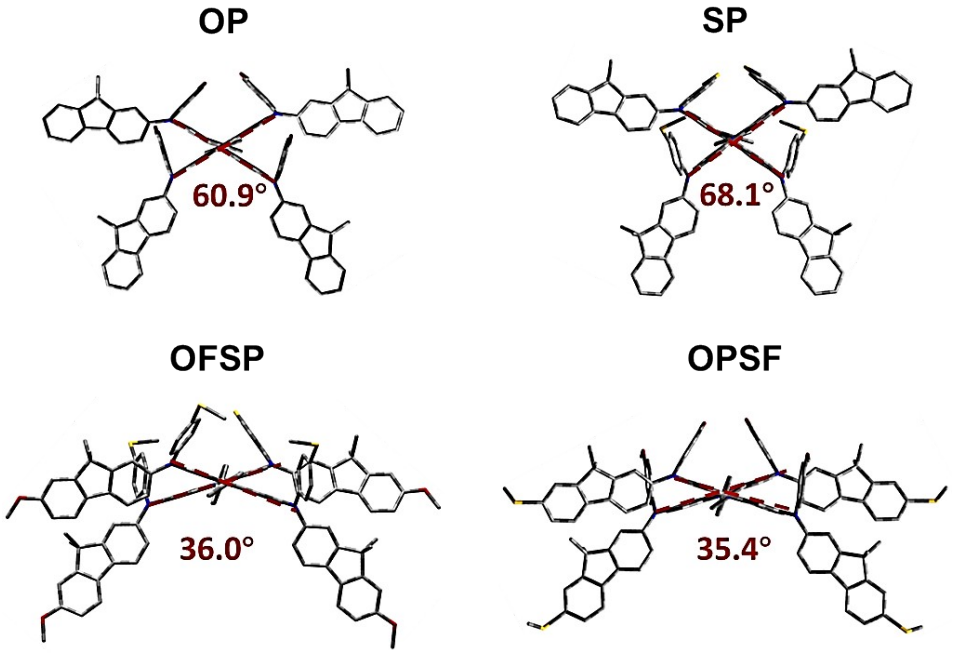

Figure S23. Optimized side view of the studied molecular ground state molecular conformation.

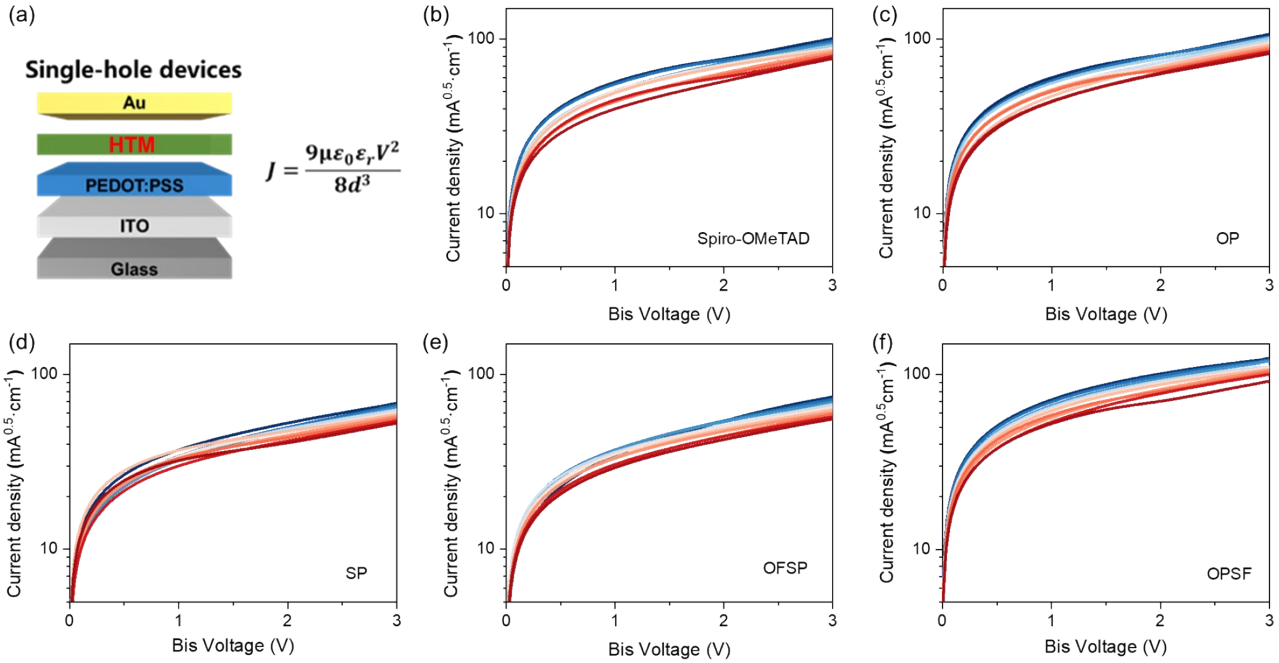

Figure S24. a) Schematic illustrations of the hole-only device and the calculation formula. *J–V* characteristics of hole-only devices based on b) doped Spiro-OMeTAD, c) doped OP, d) doped SP, e) doped OFSP and f) doped OPSF, respectively. 10 devices were fabricated for each HTM.

Hole mobility was measured by using the space-charge-limited current (SCLC) method with the device structure of ITO/PEDOT: PSS/HTM/Au[5], as shown in **Figure S24a**, where μ is the hole mobility, ε_0 is the dielectric constant of the vacuum, ε_r is the dielectric constant of the HTM, V is the bias voltage applied to the devices, d is the film thickness of the HTM.

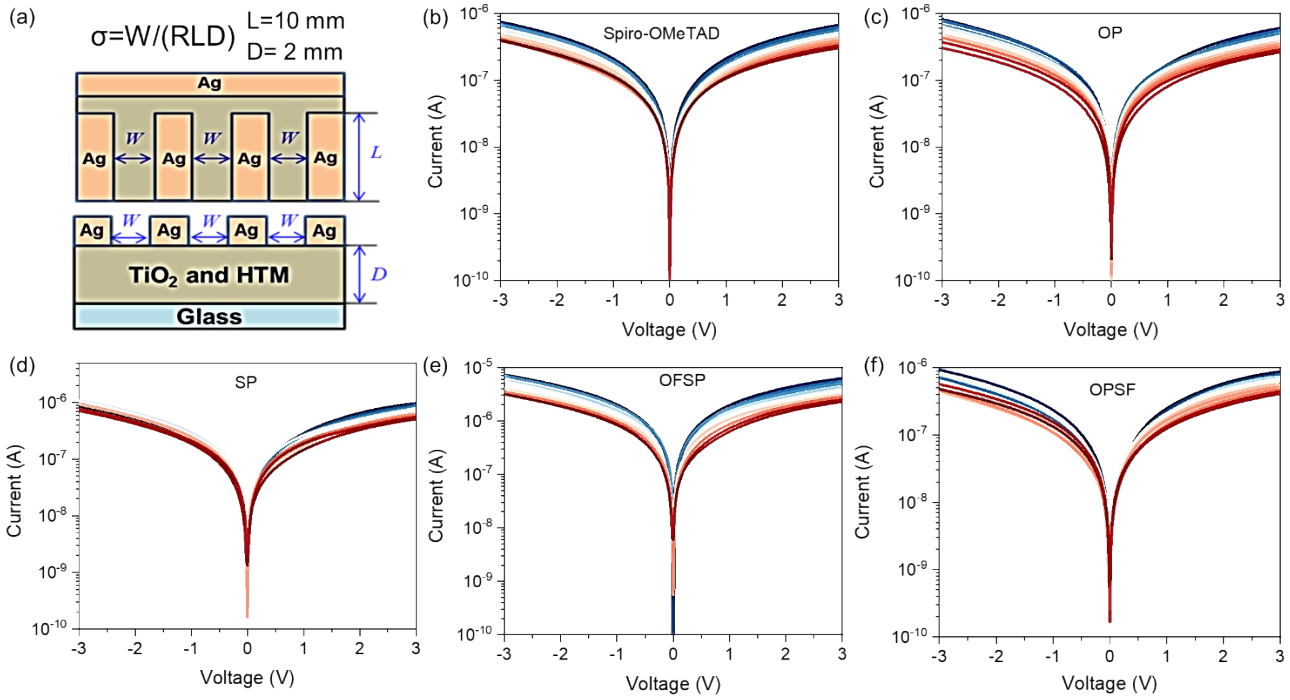

Figure S25. a) Schematic illustrations of the conductivity device and the calculation formula. Hole-conductivity characteristics of b) doped Spiro-OMeTAD, c) doped OP, d) doped SP, e) doped OFSP and f) doped OPSF, respectively. 10 devices were fabricated for each HTM.

Hole conductivities of the HTM films were determined by using two-probe electrical conductivity measurements with the device structure of Glass/m-TiO_2/HTM/Ag[6], as shown in **Figure S25a**, where L is the channel length 10 mm, W is the channel width 2 mm, D is the film thickness of the TiO_2 and HTM, and R is the film resistance calculated from the gradients of the curves.

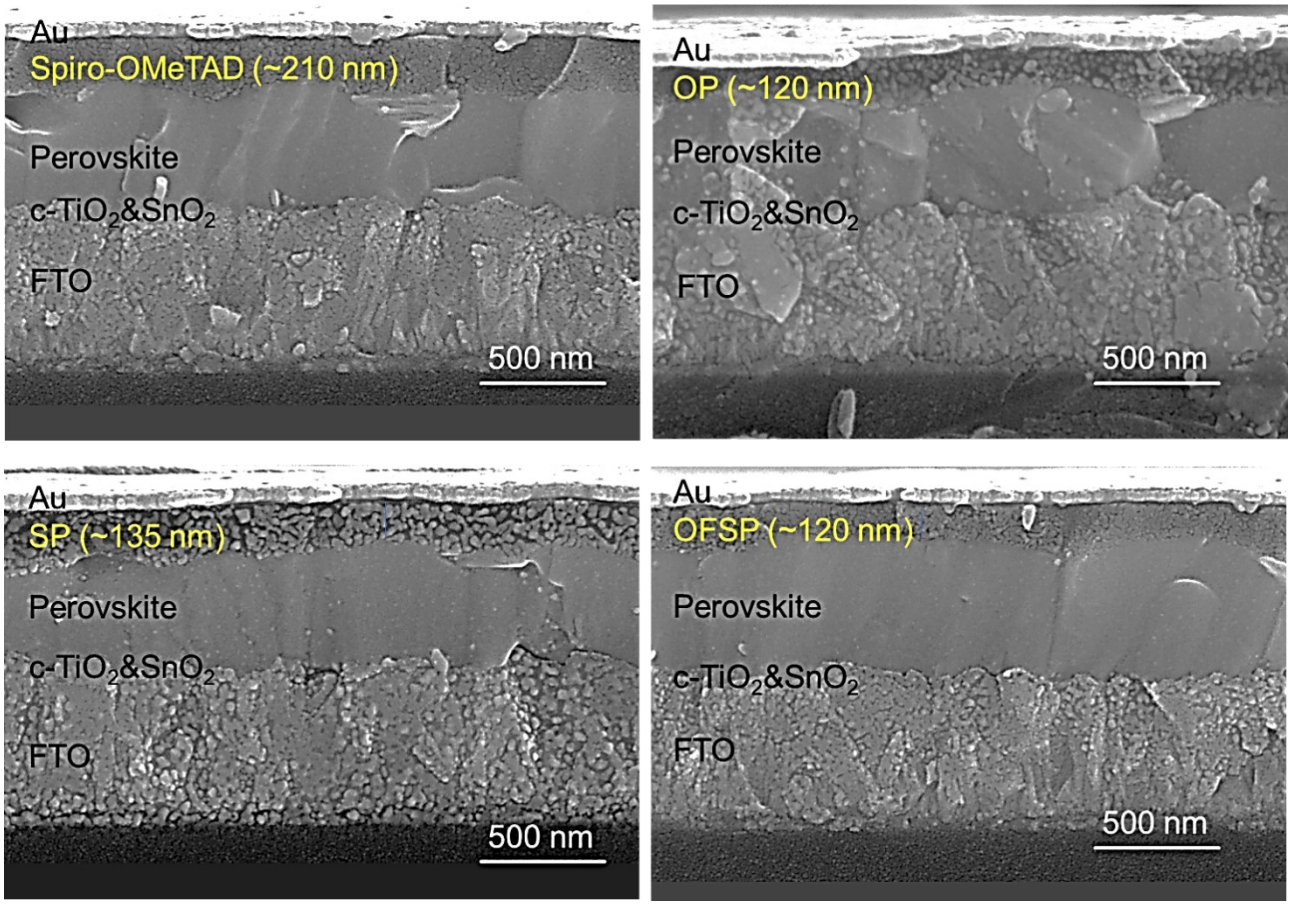

Figure S26. Cross-sectional SEM image of doped Spiro-OMeTAD, OP, SP and OFSP based device.

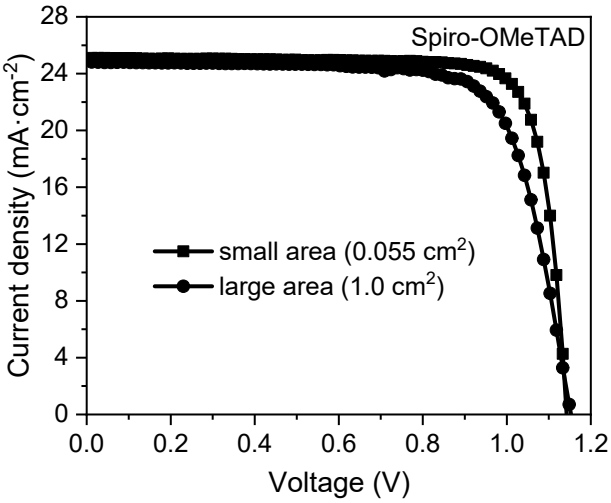

Figure S27. The champion *J*–*V* curve of small area (0.055 cm^2) and large area (1.0 cm^2) PSCs based on doped Spiro-OMeTAD.

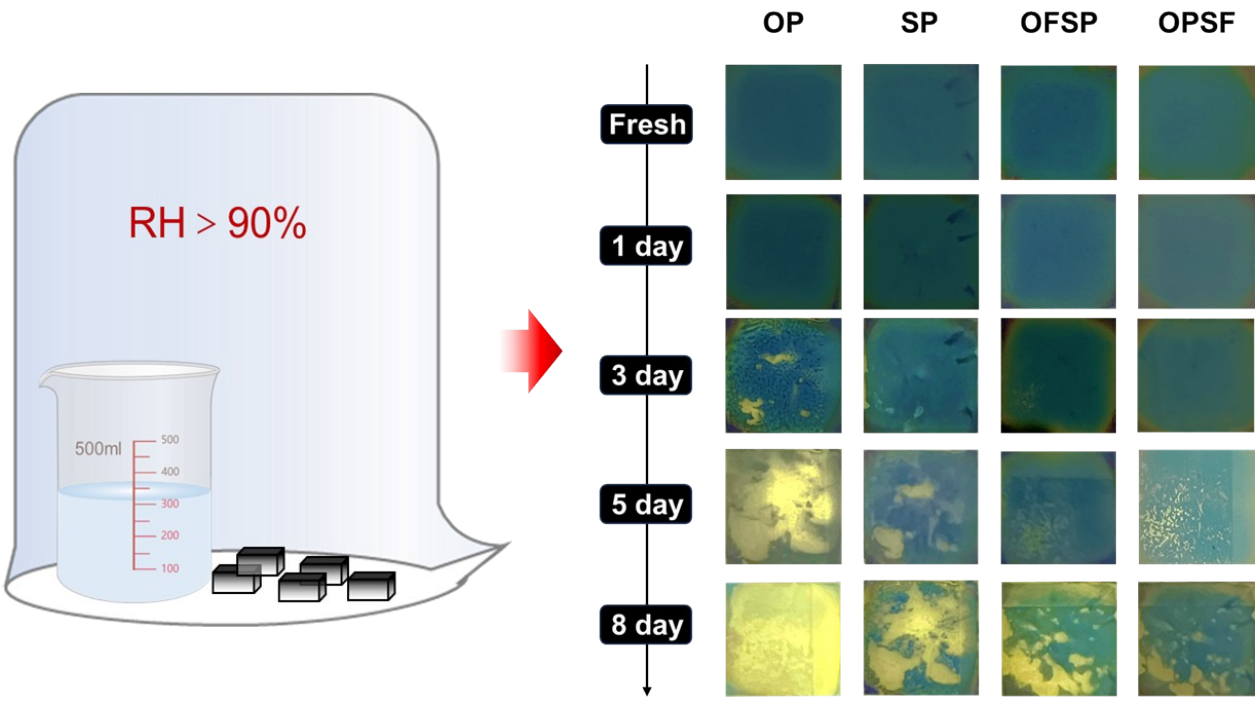

Figure S28. Degradation evolution of perovskite films covered with different HTMs under ambient conditions with room temperature and relative humidity of ＞90 %.

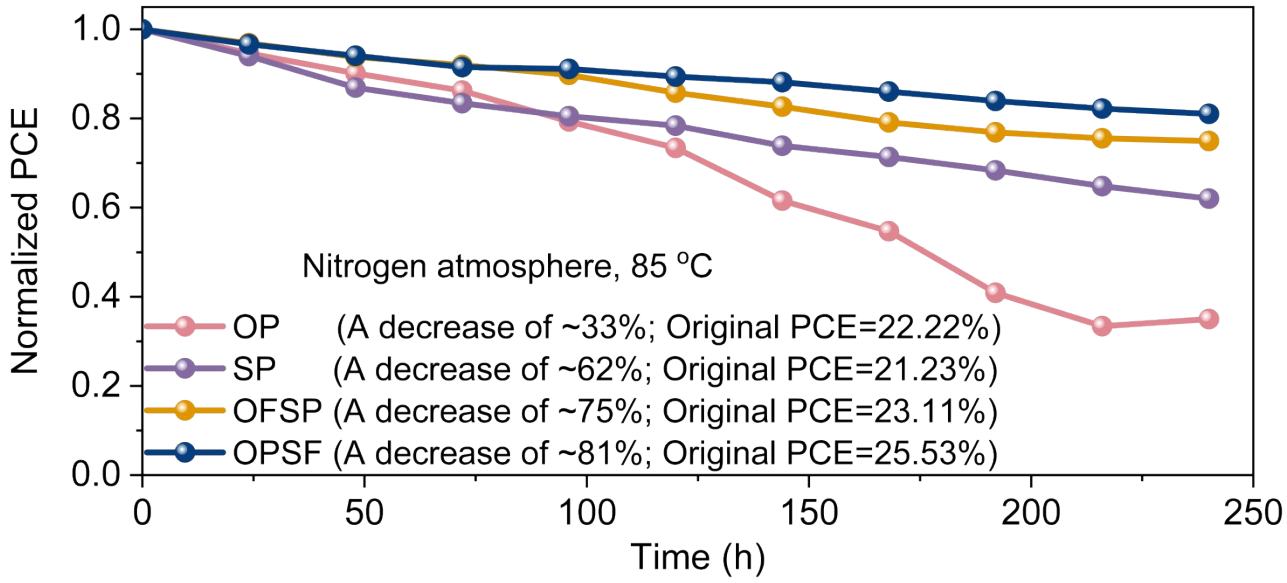

Figure S29. Normalized PCEs of devices heating at 85 °C for 240 h in N_2 atmosphere.

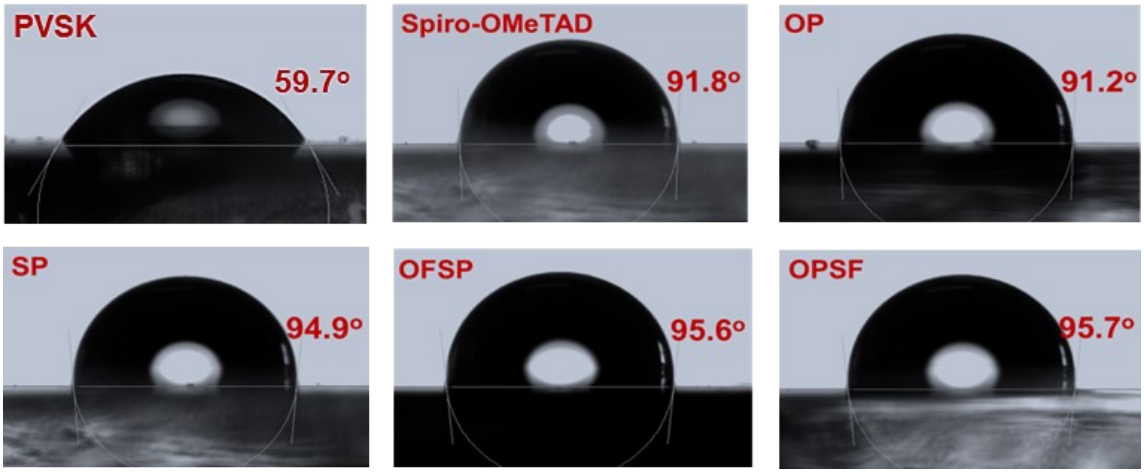

Figure S30. Water contact angles of perovskite film and perovskite films covered with doped Spiro-OMeTAD, OP, SP, OFSP and OPSF, respectively.

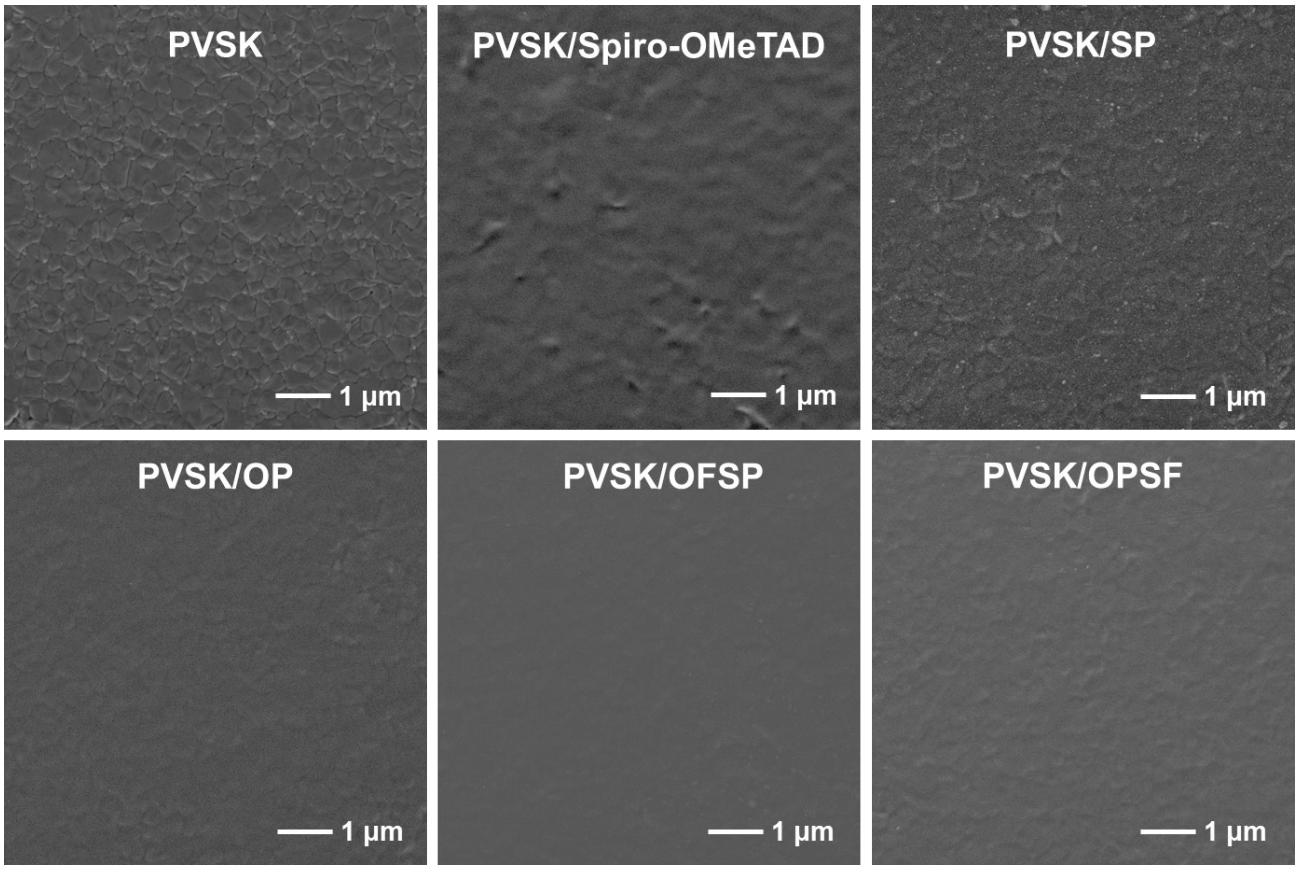

Figure S31. Top-view scanning electron microscope (SEM) images of perovskite film and perovskite film covered with doped Spiro-OMeTAD, OP, SP, OFSP and OPSF, respectively.

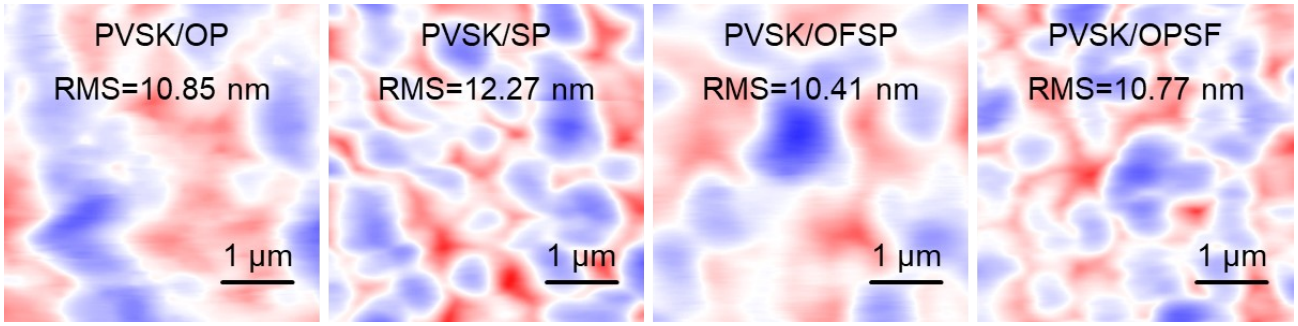

Figure S32. Atomic force microscopy (AFM) images of perovskite film covered with OP, SP, OFSP and OPSF, respectively.

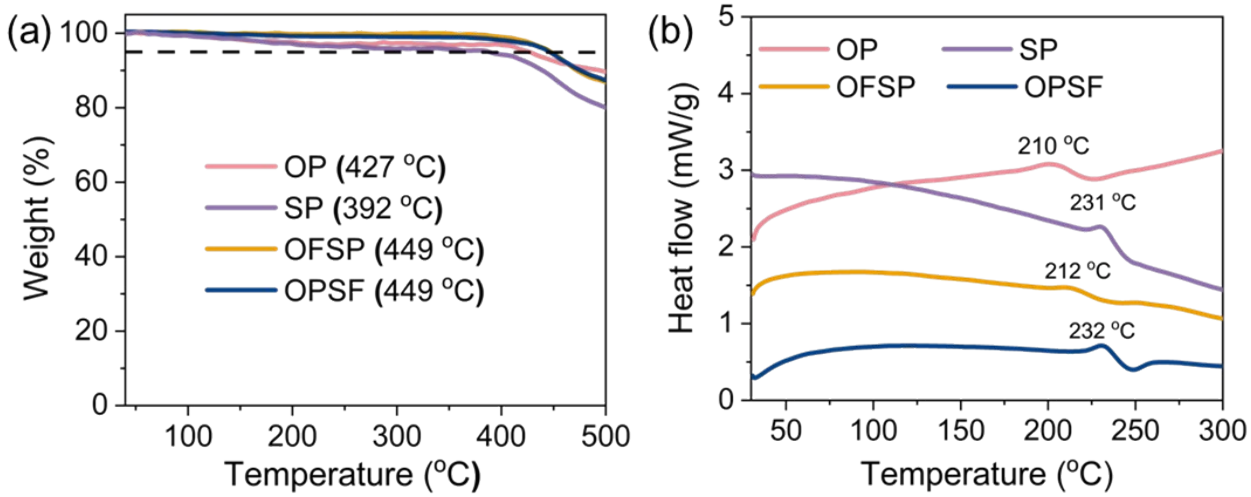

Figure S33. (a) TGA and (i) DSC curves of these studied HTMs.

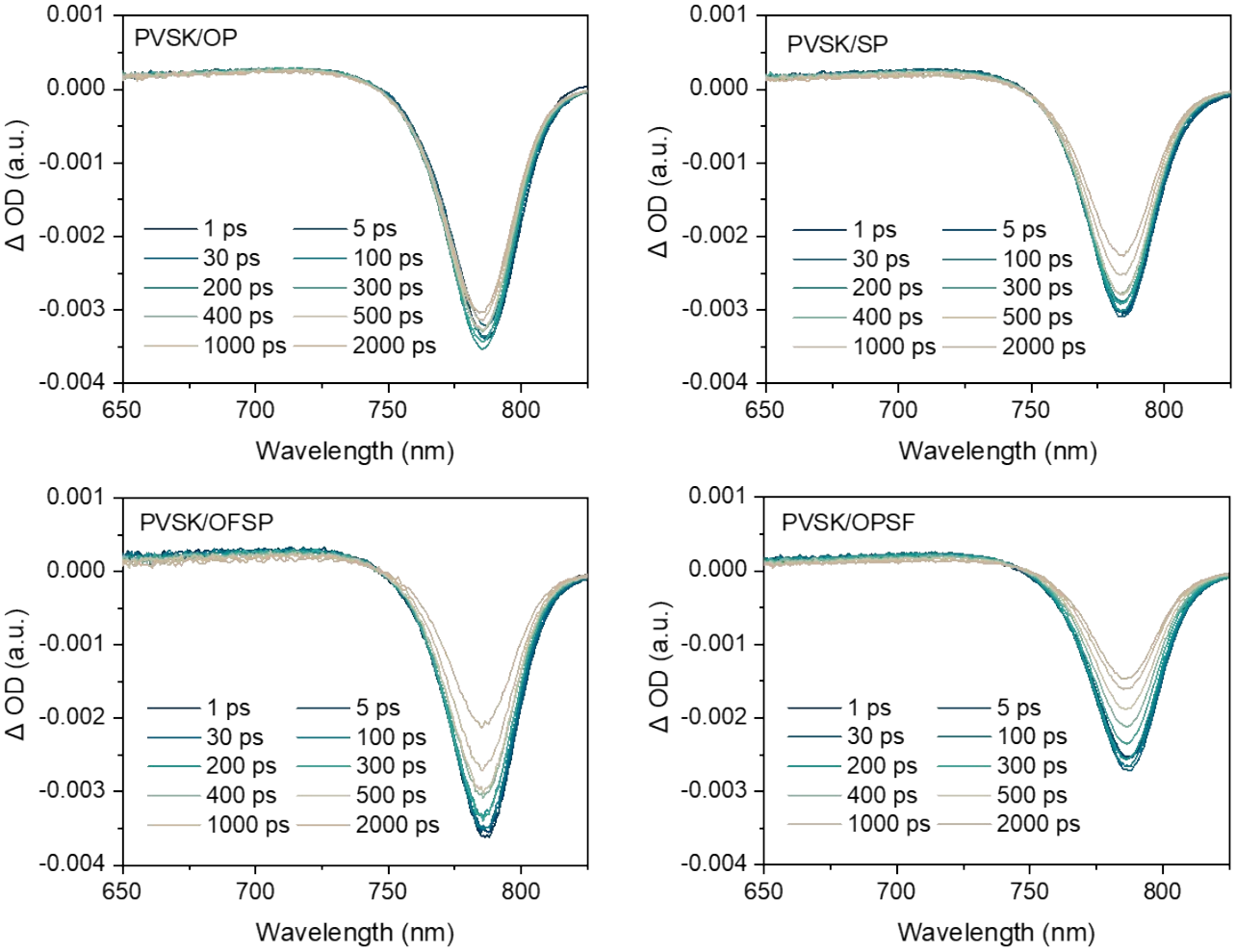

Figure S34. The fs-TA spectrum of different samples within delay time from 1 ps to 2000 ps.

6. Tables.

Table S1. Photophysical and electrochemical properties of OP, SP, OFSP and OPSF.

HTMs	$\lambda_{abs,\ max}$ (nm)	λ_{onset} (nm)	E_g (eV)	HOMO (eV)	LUMO (eV)
OP	355.8	402.6	3.08	–5.16	–2.08
SP	351.4	397.4	3.12	–5.29	–2.17
OFSP	366.5	394.9	3.14	–5.18	–2.04
OPSF	350.0	410.6	3.02	–5.20	–2.18
Spiro-OMeTAD	387.3	415.0	2.99	–5.16	–2.17

The HOMO and LUMO energy levels of the HTMs were obtained from the equation:

$$\text{HOMO (eV)} = -5.1 - (E - E_{Fc/Fc^+})$$

$$\text{LUMO} = \text{HOMO} + E_g$$

E is the first redox potential of the HTM.

Table S2. The hole mobility of doped OP.

Sample	μ ($cm^2V^{-1}s^{-1}$)	Sample	μ ($cm^2V^{-1}s^{-1}$)
1	7.07×10^{-4}	6	5.72×10^{-4}
2	6.74×10^{-4}	7	5.52×10^{-4}
3	6.32×10^{-4}	8	5.40×10^{-4}
4	5.10×10^{-4}	9	5.17×10^{-4}
5	4.69×10^{-4}	10	4.53×10^{-4}
Average: 5.63±0.85 $cm^2V^{-1}s^{-1}$			

Table S3. The hole mobility of doped SP.

Sample	μ ($cm^2V^{-1}s^{-1}$)	Sample	μ ($cm^2V^{-1}s^{-1}$)
1	2.96×10^{-4}	6	2.91×10^{-4}
2	1.46×10^{-4}	7	1.23×10^{-4}
3	1.13×10^{-4}	8	2.24×10^{-4}
4	1.64×10^{-4}	9	1.10×10^{-4}
5	2.78×10^{-4}	10	1.31×10^{-4}
Average: 1.88±0.77 $cm^2V^{-1}s^{-1}$			

Table S4. The hole mobility of doped OFSP.

Sample	μ ($cm^2V^{-1}s^{-1}$)	Sample	μ ($cm^2V^{-1}s^{-1}$)
1	3.31×10^{-4}	6	2.15×10^{-4}
2	2.90×10^{-4}	7	3.17×10^{-4}
3	2.41×10^{-4}	8	3.28×10^{-4}
4	2.86×10^{-4}	9	1.78×10^{-4}
5	2.63×10^{-4}	10	2.29×10^{-4}
Average: 2.68±0.52 $\times 10^{-4}$ $cm^2V^{-1}s^{-1}$			

Table S5. The hole mobility of doped OPSF.

Sample	μ ($cm^2V^{-1}s^{-1}$)	Sample	μ ($cm^2V^{-1}s^{-1}$)
1	6.51×10^{-4}	6	7.96×10^{-4}
2	9.56×10^{-4}	7	7.60×10^{-4}
3	5.84×10^{-4}	8	8.29×10^{-4}
4	6.89×10^{-4}	9	6.26×10^{-4}
5	9.13×10^{-4}	10	8.07×10^{-4}
Average: 7.61±1.23 $\times 10^{-4}$ $cm^2V^{-1}s^{-1}$			

Table S6. The hole mobility of doped Spiro-OMeTAD.

Sample	μ ($cm^2V^{-1}s^{-1}$)	Sample	μ ($cm^2V^{-1}s^{-1}$)
1	4.66×10^{-4}	6	3.59×10^{-4}
2	4.85×10^{-4}	7	4.43×10^{-4}
3	4.05×10^{-4}	8	4.10×10^{-4}
4	3.69×10^{-4}	9	4.18×10^{-4}
5	3.90×10^{-4}	10	4.25×10^{-4}
Average: $4.17 \pm 0.40 \times 10^{-4}$ $cm^2V^{-1}s^{-1}$			

Table S7. The hole conductivity of doped OP.

Sample	σ (S cm^{-2})	Sample	σ (S cm^{-2})
1	5.69×10^{-4}	6	5.49×10^{-4}
2	5.07×10^{-4}	7	5.61×10^{-4}
3	5.22×10^{-4}	8	5.21×10^{-4}
4	5.37×10^{-4}	9	5.09×10^{-4}
5	5.22×10^{-4}	10	5.40×10^{-4}
Average: $5.34 \pm 0.21 \times 10^{-4}$ S cm^{-2}			

Table S8. The hole conductivity of doped SP.

Sample	σ (S cm^{-2})	Sample	σ (S cm^{-2})
1	8.71×10^{-4}	6	6.18×10^{-4}
2	6.77×10^{-4}	7	6.50×10^{-4}
3	6.12×10^{-4}	8	5.98×10^{-4}
4	7.13×10^{-4}	9	6.44×10^{-4}
5	6.33×10^{-4}	10	5.91×10^{-4}
Average: $6.61 \pm 0.83 \times 10^{-4}$ S cm^{-2}			

Table S9. The hole conductivity of doped OFSP.

Sample	σ (S cm^{-2})	Sample	σ (S cm^{-2})
1	6.16×10^{-4}	6	5.94×10^{-4}
2	5.69×10^{-4}	7	5.67×10^{-4}
3	5.90×10^{-4}	8	6.06×10^{-4}
4	5.53×10^{-4}	9	5.81×10^{-4}
5	5.86×10^{-4}	10	5.56×10^{-4}
Average: $5.82 \pm 0.21 \times 10^{-4}$ S cm^{-2}			

Table S10. The hole conductivity of doped OPSF.

Sample	σ (S cm^{-2})	Sample	σ (S cm^{-2})
1	11.84×10^{-4}	6	9.64×10^{-4}
2	10.09×10^{-4}	7	11.38×10^{-4}
3	11.14×10^{-4}	8	10.25×10^{-4}
4	7.75×10^{-4}	9	11.35×10^{-4}
5	11.18×10^{-4}	10	6.82×10^{-4}
Average: $10.14 \pm 1.66 \times 10^{-4}$ S cm^{-2}			

Table S11. The hole conductivity of doped Spiro-OMeTAD.

Sample	σ (S cm^{-2})	Sample	σ (S cm^{-2})
1	4.71×10^{-4}	6	4.42×10^{-4}
2	4.46×10^{-4}	7	4.70×10^{-4}
3	4.69×10^{-4}	8	2.21×10^{-4}
4	2.46×10^{-4}	9	4.51×10^{-4}
5	4.57×10^{-4}	10	3.65×10^{-4}
Average: $4.04 \pm 0.95 \times 10^{-4}$ S cm^{-2}			

Table S12. Time-resolved PL decay fitting parameters.

Sample	τ_1 (ns)	R_1 (%)	τ_2 (ns)	R_2 (%)	τ_{avg} (ns)
PVSK	211.3	9.84	1499.7	90.16	1372.9
PVSK/OP	52.2	84.86	227.4	15.14	78.7
PVSK/SP	32.1	87.74	376.2	12.16	73.9
PVSK/OFSP	33.0	90.60	262.1	9.40	54.5
PVSK/OPSF	31.0	90.00	214.1	10.00	49.3

Table S13. The parameters of the champion PSCs based on the doped Spiro-OMeTAD.

Active area (cm^2)	V_{OC} (V)	J_{SC} ($mA \cdot cm^{-2}$)	*FF* (%)	PCE (%)	REL (%)
0.055	1.14	25.06	82.43	23.55	9.68
1.0	1.15	24.77	74.66	21.27	

Table S14. The normalized fs-TA kinetic curves fitted parameters.

Sample	τ_1 (fs)	R_1 (%)	τ_2 (fs)	R_2 (%)	τ_{ex} (fs)
PVSK/OP	304.7	49.8	303.1	50.2	303.9
PVSK/SP	250.2	49.5	244.9	50.5	247.5
PVSK/OFSP	266.8	50.3	270.7	49.7	268.7
PVSK/OPSF	215.7	50.0	215.5	50.0	215.6

$\tau_{ex} = (\tau_1 \times R_1 + \tau_2 \times R_2)/(R_1 + R_2)$

The pump of fs-TA spectroscopy with broadband capabilities and 1 fs resolution is frequency-doubled to 400 nm. The probe pulses are generated by passing another fraction of the 800 nm pulses through the 2 mm thick sapphire crystal. And then the beam of light is divided into two parts (65% forgenarate pump linght, 25% for genarate probing) through a beam splitter. linght), 65% of the energy of the light passes through the optical parametric amplifier (TOPAS) to produce 475nm prompt light and then is introduced into the ultra-fast test system (TAS). After passing through the optical delay stage, 25% of the light passes through the sapphire crystal to produce white light.

References

1. Shao, J.-Y.; Yang, N.; Guo, W.; Cui, B.-B.; Chen, Q.; Zhong, Y.-W. Introducing fluorene into organic hole transport materials to improve mobility and photovoltage for perovskite solar cells. *Chem. Commun.* 2019, *55* (89), 13406-13409.
2. Stoeck, U.; Krause, S.; Bon, V.; Senkovska, I.; Kaskel, S. A highly porous metal–organic framework, constructed from a cuboctahedral super-molecular building block, with exceptionally high methane uptake. *Chem. Commun*. 2012, *48* (88), 10841-10843.
3. Gaussian 09, Revision E.01, M. J. Frisch, G. W. Trucks, H. B. Schlegel, G. E. Scuseria, M. A. Robb, J. R. Cheeseman, G. Scalmani, V. Barone, B. Mennucci, G. A. Petersson, H. Nakatsuji, M. Caricato, X. Li, H. P. Hratchian, A. F. Izmaylov, J. Bloino, G. Zheng, J. L. Sonnenberg, M. Hada, M. Ehara, K. Toyota, R. Fukuda, J. Hasegawa, M. Ishida, T. Nakajima, Y. Honda, O. Kitao, H. Nakai, T. Vreven, J. A. Montgomery, Jr., J. E. Peralta, F. Ogliaro, M. Bearpark, J. J. Heyd, E. Brothers, K. N. Kudin, V. N. Staroverov, T. Keith, R. Kobayashi, J. Normand, K. Raghavachari, A. Rendell, J. C. Burant, S. S. Iyengar, J. Tomasi, M. Cossi, N. Rega, J. M. Millam, M. Klene, J. E. Knox, J. B. Cross, V. Bakken, C. Adamo, J. Jaramillo, R. Gomperts, R. E. Stratmann, O. Yazyev, A. J. Austin, R. Cammi, C. Pomelli, J. W. Ochterski, R. L. Martin, K. Morokuma, V. G. Zakrzewski, G. A. Voth, P. Salvador, J. J. Dannenberg, S. Dapprich, A. D. Daniels, O. Farkas, J. B. Foresman, J. V. Ortiz, J. Cioslowski, and D. J. Fox, Gaussian, Inc., Wallingford CT, 2013.
4. Xu, B.; Sheibani, E.; Liu, P.; Zhang, J.; Tian, H.; Vlachopoulos, N.; Boschloo, G.; Kloo, L.; Hagfeldt, A.; Sun, L. Carbazole-Based Hole-Transport Materials for Efficient Solid-State Dye-Sensitized Solar Cells and Perovskite Solar Cells. *Adv. Mater.* 2014, *26* (38), 6629-6634.
5. Rakstys, K.; Paek, S.; Gao, P.; Gratia, P.; Marszalek, T.; Grancini, G.; Cho, K. T.; Genevicius,

K.; Jankauskas, V.; Pisula, W.; et al. Molecular engineering of face-on oriented dopant-free hole transporting material for perovskite solar cells with 19% PCE. *J. Mater. Chem. A* 2017, *5* (17), 7811-7815.

6. Yang, C.; Wang, H.; Miao, Y.; Chen, C.; Zhai, M.; Bao, Q.; Ding, X.; Yang, X.; Cheng, M. Interfacial Molecular Doping and Energy Level Alignment Regulation for Perovskite Solar Cells with Efficiency Exceeding 23%. *ACS Energy Lett.* 2021, *6* (8), 2690-2696.